Single-cell transcriptomic analysis identifies neocortical developmental differences between human and mouse

Ziheng Zhou[1,2], Shuguang Wang[1,2,3], Dengwei Zhang[1,2], Xiaosen Jiang[1,2,4], Jie Li[1,2,4], Ying Gu[1,2,6*], Hai-Xi Sun[1,2,6*]

[1] BGI-Shenzhen, Shenzhen 518083, China

[2] China National GeneBank, BGI-Shenzhen, Shenzhen 518120, China

[3] College of Informatics, Huazhong Agricultural University, Wuhan, 430070 Hubei P.R. China

[4] BGI Education Center, University of Chinese Academy of Sciences, Shenzhen 518083, China

[5] Institute for Stem cell and Regeneration, Chinese Academy of Sciences, Beijing, 100101, P. R. China

[*] Corresponding authors: sunhaixi@genomics.cn (H.-X.S.), guying@genomics.cn (Y.G.)

Abstract

Background: The specification and differentiation of neocortical projection neurons is a complex process under precise molecular regulation; however, little is known about the similarities and differences in cerebral cortex development between human and mouse at single-cell resolution.

Results: Here, using single-cell RNA-seq (scRNA-seq) data we explore the divergence and conservation of human and mouse cerebral cortex development using 18,446 and 7,610 neocortical cells. Systematic cross-species comparison reveals that the overall transcriptome profile in human cerebral cortex is similar to that in mouse such as cell types and their markers genes. By single-cell trajectories analysis we find human and mouse excitatory neurons have different developmental trajectories of neocortical projection neurons, ligand-receptor interactions and gene expression patterns. Further analysis reveals a refinement of neuron differentiation that occurred in human but not in mouse, suggesting that excitatory neurons in human undergo refined transcriptional states in later development stage. By contrast, for glial cells and inhibitory neurons we detected conserved developmental trajectories in human and mouse.

Conclusions: Taken together, our study integrates scRNA-seq data of cerebral cortex development in human and mouse, and uncovers distinct developing models in neocortical projection neurons. The earlier activation of cognition -related genes in human may explain the differences in behavior, learning or memory abilities between the two species.

Keywords:

Cerebral cortex development, Cross-species clustering, Neocortical projection neurons, Cognition

Background

The mammalian cerebral cortex develops via a complex process of cell proliferation, differentiation, and migration events. The molecular features of the human brain at gestational weeks 7-23 are similar to those of the mouse at postnatal days 14.5 to birth (P0) and reveal gene expression differences between the two species [1, 2]. Interneurons and projection neurons, which are the two major classes of neurons, populate the neocortex. Interneurons show largely GABAergic, connecting locally within the neocortex, and are generated by progenitors in the ventral telencephalic (inhibitory cortical interneuron producing) radial glia, before migrating from sub pallial ganglionic eminences into the cortex [3-6]. By contrast, projection neurons are excitatory, which are generated by progenitors in the dorsal telencephalic (excitatory cortical neuron producing) radial glia [7-9].

Despite immense efforts over the past decades to study the cell types, function, differentiation for the mammalian cerebral cortex, especially human and mouse, large differences and conservation are observed in human versus animal models [10-12]. Elucidating the conserved, divergent and cellular architecture of developing the cerebral cortex, especially projection neurons developments, may highlight to understanding susceptibility to neurological diseases and the occurrence of cognition and memory abilities in the early stages.

Recently, with the advance of next-generation sequencing (NGS) techniques, single-cell RNA sequencing (scRNA-seq) technologies has been paved the way for study cell phenotype and cell behavior at single-cell resolution [13, 14]. More significantly, scRNA-seq can overcome the heterogeneity of cross-species analysis, bypassing the need for pure cell sorting strategies [15, 16]. Moreover, although many studies have been reported the single species cerebral cortex using scRNA-seq, there is no systematic research to

integrate the human and mouse scRNA-seq data, and compare the conservation and divergence of developing neocortex.

Here we comprehensively characterize the conservation and divergence of the cerebral cortex program between human and mouse [9, 17, 18]. We present a cross-species cell atlas and in which no obvious differences in cell type composition was observed. However, we identified different developing trajectories of projection neurons that in human the subventricular zone (SVZ) migration to deeper neocortical layers and more superficial layers are two independent processes. Additionally, the deeper and upper layers are more precisely differentiated in human than those in mouse, and lack of neuron migration signal in human. By comparing excitatory neurons gene expression across species, we also observed significant expression differences of function genes for cell migration, cognition, learning and memory in humans compared with mice. We next evaluated whether further refinement of neuronal subtypes occurs as neurons mature, indicating that human neuronal subtypes resolve from coarse laminar distinctions to refined transcriptional states in the later development, whereas mouse may not show precise subtype differentiation. In summary, we show the importance of cross-evolutionary comparison to better characterize the differences of human and mouse projection neurons development, and the relevance of these to cognition pathway. In conclusion, our study offers essential clues for researching neurodevelopment, especially for the projection neurons development, and the differences of occurrence of cognition ability in human and mouse.

RESULTS

Integration of single-cell transcriptomics of the human and mouse cerebral cortex

In order to compare cellular and molecular processes of the late corticogenesis between human and mouse, we collected published scRNA-seq data sets of human and mouse cerebral cortex at different development stages [9, 17, 18]. We reanalyzed the transcriptome profiles of 18,446 mouse neocortical cells at two key time points for corticogenesis development including 10,836 cells at embryonic day 14.5 (E14.5) from six biological replicates (Fig. 1A), and 7,610 cells at birth (P0) from three biological replicates (Fig. 1A). Because 7- to 23-post-conception-week (pcw) human brain cells are analogous to E14.5 to P0 mouse brain cells (Fig. 1A) [1, 2], we incorporated the transcriptome profiles of 6,655 human brain cells including 100 cells between 5.85 and 7 pcw, and 800 cells between 23-37 pcw (Fig. 1A). To ensure that cells from different species and data sets can be properly integrated, we performed unbiased clustering using Uniform Manifold Approximation and Projection (UMAP) [19]. The major cell lineages in cerebral cortex such as excitatory neurons, inhibitory neurons, neuronal progenitor cells and glial cells were able to be identified using their lineage markers [20, 21] (Fig. 1B, C). Moreover, there was no obvious bias because the majority of the cell types could be identified in all three data sets (Fig. S1C).

Because the number of mouse cells (18,446) was about 3 times higher than that of human cells (6,655) which may cause bias, we randomly extracted 6,655 mouse cells in further analysis. Finally, 13,278 cells (6,655 mouse cells and 6,623 human cells) were used (Fig. 1A) in further analysis which covers all major cell types (Fig. 1D, E).

Identification and characterization of cortical cell types

127 We first compared the cell composition and found that mouse had more interneuron than
128 human (Fig. 2A). We next compared the cell number in each cluster and found that cluster
129 06 Inh_striatal and cluster 09 Layer [19P] had more cells in mouse (20%-30%) than in
130 human (70%-80%). In contrast, cluster 16 Microglia and 17 Mesenchyme had more human
131 cells (80%-90%) (Fig. 2B).
132
133 We next examined the correlation among clusters by cross-species clustering (Fig. 2C).
134 As there were still considerable species differences between humans and mice, we used
135 the integrated matrix. Remarkably, excitatory neuron exhibited a profile highly similar to
136 interneuron, and Glia showed itself a high degree of correlation (Fig. 2C). Interestingly,
137 Cluster 16 Microglia were distinct from excitatory neuron, interneuron and other Glia cells
138 (Fig. 2C). We also calculated the correlation using human and mouse cells respectively
139 and found that human and mouse had similar results with cross-species (Fig. S2A, B).
140
141 We checked the top 10 highly expressed genes of each cluster and found most of them
142 were consistent among human and mouse (Fig. 2D, S2C, D). For example, two SVZ
143 clusters (Clusters 00 SVZ and 01 SVZ) were featured by predominant expression of
144 *EOMES* (*TBR2*) and *ZBTB20* [22-24]. Cells in Cluster 01 SVZ also expressed markers of
145 both excitatory (*NEUROD6*) and inhibitory (*CALB2*) neurons [25-27] which exhibited the
146 expression patterns of rostral migratory steam [18]. Cells in deep-layer populations
147 (Clusters 02 Exc deep and 03 Exc deep) exhibited high expression levels of *BCL11B* [28].
148 Cells in Clusters 04 Exc upper and 05 Exc upper expressed upper layer marker *MEF2C*
149 [8, 29]. We identified *NEUROD6* and *NEUROD1* kept consistently high expression in
150 excitatory inhibitory, and *EOMES* expressed in subventricular zone (SVZ), and *STMN2*
151 expressed strongly in deep and upper layer and increased the levels of expression with
152 neuron maturation, which conversed the transformation known genes expression
153 trajectories in neurogenesis among human and mouse (from *EOMES* to *STMN2*) [9, 30]

154 (Fig. 2D). Three interneuron clusters (Clusters 06 Inh_striatal, 07 Inh and 08 Inh) were
155 characterized by expression of *GAD2* and *NRXN3*. Specifically, in Cluster 08 Inh we found
156 high expression of *LHX6*, *SST* and *MAF* indicating 08 Inh is somatostatin (SST)
157 expressing interneurons but not parvalbumin (PV). *LHX6* is a transcription factor
158 associated with PV and SST interneuron [31, 32], whereas *SST* and *MAF* regulate the
159 potential of interneurons to interneurons to acquire SST+ interneuron identity [33].
160 Interneuron migrate tangentially from the ganglionic eminences, and ganglionic
161 eminences (Cluster 13 GE) expressed high levels of inhibitory marker *DLX1* and
162 proliferation markers *TOP2A* and *MKI67* [34]. RG marker *HES5* was in two RG clusters
163 (Clusters 10 RG and 11 RG), while Cluster 11 RG expressed high levels of *MKI67* and
164 *TOP2A* genes. We also found *GAP43*, a key regulator in early brain development, was
165 constitutively expressed in all these cell types in both human and mouse [35].
166
167 We identified Clusters 06 Inh_striatal and 09 Layer[19P] as inhibitory neurons and they
168 had similar gene expression patterns and cell numbers in human and mouse. Striatal
169 inhibitory neurons (Cluster 06 Inh_striatal) expressed inhibitory markers *GAD2* and lower-
170 layer marker *BCL11B* [36]. Layer 19-P (Cluster 09 layer[19P]) expressed canonical Cajal-
171 Retzius cell markers *RELN* and Purkinje cell marker *PCP4*. In addition, they also
172 expressed non-coding RNAs *SNHG11* and *MEG3* (Fig. 2D, S2C). Microglia (Cluster 16
173 Microglia) had higher cell numbers in human than in mouse and exhibited low expression
174 correlation with other clusters. They expressed microglial markers such as *LAPTM5*,
175 *C1QA*, *C1QB*, and *C1QC* [37], as well as several microglia-specific pathways such as
176 TREM2-TYROBP pathway [37-40] (Fig. 2D). Interestingly, Cluster 20 Unknown exhibited
177 an intermediate state between excitatory neuron and interneuron: it had high expression
178 correlation with both excitatory neuron and interneuron, and expressed several marker
179 genes such as *STMN2* (excitatory neuron) and *NNAT* (interneuron) (Fig. 2D, S2C, D).
180
181 **Different developmental trajectories of excitatory neuron between human and**

182 **mouse**

183

184 To compare the developmental trajectories in excitatory neuron between human and
185 mouse, we split the data into 6,623 human cells and 6,655 mouse cells, and performed
186 unbiased clustering using UMAP again. We identified 23 clusters and also observed
187 lineage separation of the major cell types (Fig. S3A, B, C, D). We used *NEUROD6* as
188 marker gene and identified 6 excitatory neuron clusters in human (Cluster 00 SVZ, 01 Exc
189 deep, 02 Exc deep, 03 Exc upper, 04 Exc upper and 05 Exc upper) and 7 excitatory neuron
190 clusters in mouse (Cluster 00 SVZ, 01 SVZ, 02 Exc deep, 03 Exc deep, 04 Exc deep, 05
191 Exc upper and 06 Exc upper) (Fig. S3A, B). We then reconstructed the corticogenesis
192 developmental trajectories using Monocle analysis. Both human cells and mouse cells
193 were distributed along pseudo-temporally ordered paths from SVZ to neocortical layers,
194 including deeper neocortical layers (layer VI, then layer V) and superficial layers (layer IV,
195 then layer II/III) [28] (Fig. 3A, B). Surprisingly, we found that the developmental trajectory
196 in mouse was a continuous process without any branch, in which SVZ migrated to deeper
197 neocortical layers and then to superficial layers. By contrast, in human this process had
198 two branches in which SVZ migrated to both deeper neocortical layers and superficial
199 layers (Fig. 3A, B, S3E, F). Consistent with this observation, we found that SVZ marker
200 *EOMES* was specifically expressed in the beginning of trajectories, deep-layer marker
201 *BCL11B* was specifically expressed in the upper branch in human, whereas migratory and
202 upper-layer markers *POU3F2* and *SATB2* were specifically expressed in the lower branch,
203 which was different from those in mouse trajectory (Fig. 3A, B, S3I). More important, when
204 we further split the data based on development stages, we still found that the lower-layer
205 neurons were present in 7 to 23 pcw in human and E14.5 and P0 in mouse, with high
206 expression of *BCL11B*. Meanwhile, a large number of Layer II-IV (upper layer) cells at P0
207 in mouse and 20-23 pcw in human was identified, with high expression of *SATB2* (Fig.
208 S3G, H).

209

210 We identified 109 differentially expressed genes in human that may determine cell fate
211 commitment. They were fall into 4 clusters which exhibited successive waves of gene
212 expression in different branches (Fig. 3E). In addition, Gene Ontology (GO) enrichment
213 analysis revealed that the functions of genes predominantly expressed at the SVZ branch
214 were enriched in cerebral cortex development, olfactory bulb development and olfactory
215 lobe development as previously reported [41]. Among these genes, transcription factor
216 *PAX6* is crucial for SVZ neurogenesis and also acts via retinoid signaling to regulate eye
217 development [42] suggesting that eye development may have relative to SVZ
218 neurogenesis (Fig. 3E). Lower-layer from human cortex showed increased expression of
219 genes for modulation of synaptic signaling and chemical synaptic transmission, which
220 have a mechanistic link with learning and memory by plasticity regulation [43]; whereas
221 upper layer CPN from human cortex exhibited increased expression of genes involved in
222 regulation of sodium ion transport and calcium-mediated signaling (Fig. 3E). Genes
223 related to forebrain neuron fate commitment and forebrain neuron differentiation were
224 expressed in both lower-layer and upper layer. More interestingly, the functions of genes
225 that were highly expressed in SVZ, lower layer and upper layer were all enriched in
226 cognition and learning (Fig. 3E).

227

228 We further analyzed the migratory marker genes expression in neocortical. We found
229 these genes had continuously increased expression in SVZ, and decreased expression in
230 deep-layer and upper-layer in human. Specifically, *NRP1* and *PALMD*, which were
231 involved in the regulation of cell morphogenesis and cerebral cortex cell migration,
232 exhibited increased expression in the SVZ lineage and then declined in deep layer and
233 upper layer lineage, suggesting that neuronal migration in projection neurons in the
234 cerebral cortex may occur from the SVZ's maturity stage to the early development of deep
235 and shallow layers, rather than the late deep layer [44] (Fig. S3J, K). By contrast, in mouse

236 cerebral cortex we found migratory genes showed increased expression in SVZ and deep
237 layer, and decreased expression in upper layer suggesting that in mouse the deep layer
238 continuously process cell migration from SVZ to upper layer. Representative genes
239 include *Meis2*, *Nrp1* and *Pou3f2*, whose functions are relative to cell migration and
240 regulation of cell morphogenesis involved in differentiation (Fig. S3K).
241
242 **Divergence in neocortical between human and mouse**
243
244 In order to better understand the distinct layers in neocortical in human and mouse, we
245 performed a comparison of cortical expression models through single-cell analysis,
246 including deeper neocortical cortex (layer VI, then layer V) and late-born neurons migrate
247 through deep layers to gradually fill more shallow layers (layer IV, then layer II/III). Pairwise
248 comparison of human and mouse cortical layer data sets identified a large number of
249 differentially expressed genes (DEGs) (Fig. 4A). We observed a considerably bigger
250 number of differentially expressed genes in human than in mouse, meanwhile we also
251 found some co-expression marker genes, for example, fez family zinc finger 2 *Fezf2* (high
252 expressed in deeper layers), special AT-rich sequence binding protein 2 (*SATB2*) and
253 *POUEF2*, a marker of layer II/III with function of migration and differentiation [28]. More
254 interestingly, we detected the differentially expressed gene: *CLSTN2*, high expressed in
255 human deep layer and mouse upper layer, which significantly associated with pathway of
256 cognitive and memory behavior and reduction in functional inhibitory synapses [45],
257 suggesting that genes, relating to cognition and memory pathways, expressed earlier in
258 human than mouse.
259
260 Pathway analysis of two layers specific to humans revealed enrichment of axon
261 development, such as axon guidance and axonal fasciculation, compared with mouse (Fig.
262 4B). Additionally, enriched pathway contained in many aspects, including visual system,

263 facial nerve, trigeminal nerve and motor neuron in human — more specifically, retinal
264 ganglion cell axon guidance, facial nerve development, trigeminal nerve development,
265 motor neuron axon guidance and regulation of synaptic transmission, glutamatergic (Fig.
266 4C). In contrast, some pathways were enriched in mouse, mainly in cell fate commitment,
267 neuron fate commitment and neuron migration (Fig. 4C).
268
269 To continuously process research in neocortical in human and mouse, we expanded our
270 analysis included SVZ. Pairwise comparison of human and mouse SVZ and upper cortical
271 layers scRNA-seq transcriptomics data identified a large number of DEGs (Fig. S4A). The
272 number of DEGs detected in mouse was 6 times higher than that derived from human.
273 SVZ marker genes, *EOMES* and *NHLH1*, related to cell-type determination within
274 developing neurons, upper layer markers, *SATB2* and *MEF2C*, had co-expression in
275 human and mouse. We found more than 200 significant gene ontology (GO) terms in
276 human and mouse respectively. Specifically, for human, pathways focused on neuron
277 migration and axon development. In addition, human-specific genes also revealed
278 enrichment of “eye development”, “visual system development”, and “sensory system
279 development”. For mouse, we detected mouse-specific pathways “learning or memory”,
280 and “synapse organization” (Fig. S4B). we also identified the DEGs between SVZ and
281 deeper layer among human and mouse (Fig. S4C). The number of DEGs are equal in
282 human and mouse (Fig. S4D).
283
284 We next examined the correlation between each cluster in neocortical between human
285 and mouse (Fig. 4D). We identified mouse SVZ and mouse upper layer showed
286 remarkably low degree correlation (Fig. 4D). In contrast, the correlation of human SVZ
287 with human deep layer were nearly similar to those of human SVZ with human upper layer
288 (Fig. 4D). Taken together, we conclude that the differences of deeper layer and upper layer
289 has larger in human than mouse, while the differences of SVZ and upper layer has larger

290 in mouse than human (Fig. 4D).

291

292 Having defined the populations of SVZ, deeper layer and upper layer cells, we further used
293 CellPhoneDB to perform an unbiased ligand receptor interaction analysis between these
294 populations [46]. To detect how neocortical projection neurons are generated in human,
295 we focused functional analyses on interactions with SVZ, deeper layer and upper layer
296 (Fig. 4E). SVZ expressed *PTN* and *MDK*, signaling to receptors *ALK* on upper layer, that
297 are known to regular nervous system development, function, and repair, especially,
298 regulating the sympathetic neuron growth during development and aberrant signaling to
299 neuroblastoma predisposition [47-49] (Fig. 4E). SVZ expressed *PTN* and *MDK*, signaling
300 to the receptor tyrosine phosphatase family *PTPRZ1* on deeper and upper layers, which
301 shows the significant function in activate cell growth, migration and cellular activities (Fig.
302 4E). More importantly, *PTPRZ1* interaction with *MDK* promotes neuron migration [50]. SVZ
303 expressed high levels of *NOTCH3* interacting with receptor *DLL3* on deeper layer cells
304 and upper layer cells, which could modulate cellular differentiation, fates for terminal
305 neuronal differentiation and links to progression toward a neuronal fate in the developing
306 cortex [51, 52](Fig. 4E). In addition, ephrin family showed high level of expression in
307 human cortical. Firstly, *EPHA8_EFNA5* could promotes neurite outgrowth and axon
308 guidance [53], which showed significance in process SVZ to deep layer (Fig. 4E).
309 *EFNA1_EPHA4* involves in dendritic spine morphogenesis in deep layer to upper layer
310 [54] (Fig. 4E). Deep layer expressed *WNT* genes interacting with receptors *FZD4* and
311 *ROR1* on upper-layer cells. *WNT5A_ROR1* promotes the formation of presynaptic [55]
312 (Fig. 4E). Upper layer expressed Atypical Chemokine Receptor 2 ligands (*ACKR2*)
313 receptors that are known to be required for immature/mature dendritic cells [56] (Fig. 4E).
314 *ESAM_ESAM* helps cell-cell adhesion in deep layer to upper layer (Fig. 4E).

315

316 In summary, our trajectory, cell-type and unbiased ligand-receptor interactions analysis

317 between mouse and human indicates that human and mouse have differences in
318 development neocortical models, the correlation between deep layer and upper layer are
319 lower in human than mouse, and the ligand-receptor analysis indicate that deep layer and
320 upper layer may not have various neuron migration interactions in human. These
321 phenomena may therefore show SVZ migration to appropriate layers are relatively
322 independent in human neocortical projection neurons.
323
324 **Characterization of the excitatory neuron gene expression pattern across species**
325
326 To better understand the divergence and conservation of excitatory neuron gene
327 expression across evolution, we used developmental time course reconstructed by
328 monocle analysis to process the further analysis of gene expression pattern. Although a
329 large part of genes keep conservation across evolution, some genes showed converse
330 expression trends in human and mouse. We defined two gene expression clusters, with
331 cluster a representing up-regulated genes during the frontal development excitatory
332 neuron in human, mainly including SVZ cells (Fig. 5A), and in mouse, the expression
333 patterns are converse (Fig. 5B). Cluster a contained genes *VCAN*, *BCL11B*, *SOX5*, *PTN*
334 and *CNR1*, whereas Cluster b contained genes *ST18*, *KLHL13* and *NHLH2* (Fig. 5A, B).
335 We focused some genes have key functions in neuron development, for example, we
336 detected *CNR1* have various difference in expression pattern, in human, it expressed in
337 SVZ cells, whereas it expressed in deeper and upper layer cells in mouse, in other words,
338 CNR1 expressed earlier in human than mouse in cortex (Fig. 5A, B, C). CNR1, known as
339 cannabinoid receptor 1, is expressed in the peripheral nervous system and central
340 nervous system and combine cannabinoid to regulate the release either glutamate or
341 GABA, and the endocannabinoids (*eCBs*) and their receptors (*CNR1*) express in cortex
342 that can act as the significant function as cell proliferation and migration and axon
343 guidance during the critical stages of brain development [57-62]. In addition, *CNR1* also

344 likely plays an important role in the development of memory and cognition, and is relative
345 to many emotional, neurological diseases, such as novelty [63-65]. *ST18*, expressing
346 earlier in mouse than human, shows key factor in breast cancer [66] (Fig. 5A, B, D).
347
348 In order to detect the function of cluster a genes and cluster b genes, we found more
349 genes with similar expression patterns to process GO terms, function protein network and
350 transcriptional regulatory relationships analysis. We detected some neuron differentiation
351 and synaptic pathways, including chemical synaptic transmission, cell morphogenesis
352 involved in neuron differentiation, active in human SVZ (Fig. S5E, F). More interesting,
353 axon development, learning or memory, neuron recognition, cognition, regulation of
354 behavior and regulation of synaptic transmission, glutamatergic were more active in the
355 human SVZ than mouse SVZ (Fig. 5E). The key genes, enriching in cognition, learning or
356 memory, neuron differentiation and neuron regeneration pathways, including *PTPRZ1*,
357 *PTN*, *CNR1*, *ATP1A2*, *SOX5* and *JUN*, showed the different expression pattern in human
358 and mouse excitatory neuron, suggesting human probably develop these function,
359 especially for cognition, learning or memory, earlier than mouse (Fig. 5F, S5A, B, C, D).
360 According to protein and transcription factor analysis, we observed key protein or
361 transcription factor: *JUN* connected with *FOS*, as a classic marker for neuronal activation,
362 which has important regulator of axonal regeneration and neuronal activation. [67] (Fig.
363 5A, 5B, S5E, F). Moreover, *JUN-PTN* was detected TF-target regulatory relationship,
364 which directly indicated activation of neuronal migration during later brain development
365 [68-70], and ligand-receptor interaction: activating *PTN_PTPRZ1* in human SVZ to deeper
366 layer and SVZ to upper layer before (Fig. 4E), which activates cell growth, migration and
367 cellular activities [70, 71], and we found these genes have different expression pattern in
368 human and mouse, for human, they showed highly expression in SVZ, whereas *Ptprz1*
369 and *Ptn* performed low expression in mouse SVZ, and increase expression in deeper layer
370 and upper layer cells (Fig. 5A, B, S5A, B), indicating that neuron cell migration performs

371 in human SVZ to deeper layer and upper layer or mouse deeper layer to upper layer
372 process. We also found genes expressing in mouse SVZ, like *ST18* and *UACA*, relative
373 to reactive oxygen species biosynthetic process (Fig. 5D, E).
374
375 **Single-cell transcriptomic analysis identifies human excitatory neuron subsets**
376
377 In order to examine whether the excitatory neuron of human and mouse display similar
378 cell types or contain several subtypes, we further observed the clustering of human and
379 mouse (Fig. S3A, B). Surprisingly, distinct clusters of maturing neurons (04 Exc upper and
380 05 Exc upper) reproducibly emerge according to the distinct expression profiles, including
381 reciprocal expression of PFC (The prefrontal cortex) marker (*ABCA1*) and V1 (Visual
382 cortex) marker (*LPL*) [9] (Fig. 6A). By contrast, the gene with reciprocal expression in
383 human 04 Exc upper and 05 Exc upper don't have similar expression patterns in mouse
384 (Fig. 6B).
385
386 In order to further make sure the cell types, we used known labels to tag the clustering
387 and processed statistics (Fig. S6A, B, C, D), we found that the proportion of PFC and V1
388 cells have remarkable difference in 05 Exc upper (Fig. S6C), suggesting that the coarse
389 laminar distinctions among newborn neurons are resolved into refined transcriptional state
390 in human later development, whereas the phenomenon disappeared in cross-species
391 clustering that the number of PFC and V1 cells in each cluster are similar, especially in
392 excitatory neuron, indicating that the newborn neurons probably don't have refined
393 expression states in mouse among the E14.5 and P0 stages (Fig. S6D).
394
395 In order to detect the biological processing of PFC and V1 in human, We therefore selected
396 expression differentially genes for pathway analysis by gene ontology resource and
397 functional protein association networks (STRING) [72](Fig. 6C, S6D, E, F). Axon guidance,

398 axonogenesis, axon development were active in PFC and V1 (Fig. 6C). Pathway relative
399 to synapse signaling, including synapse organization, modulation of chemical synaptic
400 transmission, regulation of trans-synaptic signaling and synapse structure or activity,
401 synapse maturation, axonal transport of mitochondrion, were more active in V1 (Fig. 6C).
402 In PFC area, we enriched sensory system development and cognition, rather in V1, and
403 in PFC and V1, we all discovered visual system development and eye development (Fig.
404 6C).
405
406 To further examine the notion of typological distinction between PFC and V1 inner human
407 and mouse, we compared distinct co-expression profiles of genes involved in the
408 specification of projection patterns during development, for example, *SATB2* and *BCL11B*
409 co-expressed in human maturing PFC deep layer and upper layer at later stages of
410 development (Fig. 6D). In contrast, neurons in V1 had distinguish expression pattern of
411 *BCL11B* and *SATB2* (Fig. 6D). More interestingly, *Bcl11b* and *Satb2* also had co-
412 expression phenomenon in mouse, but it appeared in the immature neurons, indicating
413 that the early fate specification [18] (Fig. 6D). Then, we found that it is common that
414 maturing PFC neurons co-expressed genes in deeper and upper layer cells, for example,
415 *ABCA1* and *VCAN*, which couldn't express in deep layer in mouse (Fig. 6E, F). Additionally,
416 we focused on the function of these genes, which may play role in intercellular signaling
417 and extracellular structure organization.
418
419 **Conservation of radial glia developmental trajectories**
420
421 The comparison of excitatory neurons is crucial for our understanding of many differences
422 between human and mouse developing cortex. However, they are many cell types that
423 haven't been compared. We further analyzed the developmental trajectories in radial glia.
424 We observed there are two RG clusters in cross-species clustering (cluster 10 RG and 11

425 RG) (Fig. 1D), which had similar human and mouse cells proportions (Fig. 2A, B). During
426 early development, dorsal telencephalic radial glia produces excitatory cortical neurons,
427 while ventral telencephalic produces inhibitory cortical interneuron during 7 to 23 pcw in
428 human that have been reported [9]. We applied principal component analysis (PCA) for
429 cross-species clustering that observed 11 RG migrate to 13 GE (Interneuron migrate
430 tangentially from the ganglionic eminences) and 12 G2/M, and 10 RG migrate to 00 SVZ
431 (Fig. S7A, B), and then, we chose these clusters to reconstruct the trajectories analysis
432 (Fig. 1D), that we found two lineages: from 11 RG to 13 GE and 12 G2/M or 10 RG to 00
433 SVZ (Fig. 7A). Group of cells expressing *MKI67*, markers of proliferating and glia, were
434 detected at early timepoint at the pseudo-time analysis by Monocle, while *EOMES* and
435 *NEUROD6* expressed in SVZ branch, and *GAD2* expressed in GE branch (Fig. 7B). We
436 detected that these developing processes have been emerged at stage 2 (E14.5 in mouse
437 and 7- to 11.5 pcw in human). We use species-specific clusters to analysis with four
438 markers to depict the expression profile (Fig. S7B, C, D, E).
439
440 In order to detect the gene expression relative to cell fate commitment, we identified 80
441 genes highly dispersed in human and mouse. DE genes that fall into 5 clusters and
442 depicted successive waves of gene expression in different branches (Fig. S7F). Genes
443 predominantly expressing at the 11 RG branch enriched in pathways, including nuclear
444 division, mitotic nuclear division and sister chromatid segregation, suggesting that these
445 cells stayed in G2/M stages (Fig. S7F). Genes co-expressed in 10 RG and 11 RG enriched
446 in epithelial cell proliferation, gliogenesis, astrocyte differentiation, as expected in radial
447 glia (Fig. S7F). GE cells expressed genes, relating to cerebral cortex GABAergic
448 interneuron differentiation (Fig. S7F).
449
450 To examined two RG expression profile and enrichment pathways in human and mouse,
451 we detect expression differentially genes in these two clusters (Fig. 7C). 11 RG expressed

452 some proliferating marker genes, including *MKI67*, *TOP2A* and *UBE2C*, and regulate cell
453 cycle genes, like *CDK1* and *TPX2*, which co-expressed in human and mouse ventral
454 telencephalic radial glia (Fig. 7C); while dorsal telencephalic radial glia expressed three
455 kinds genes, *HES5* (RG marker), *EOMES* (SVZ markers) and *DACH1* (enriched in
456 ventricular radial glia cells) [73] (Fig. 7C), that related to olfactory bulb development and
457 olfactory lobe development, which also enriched in SVZ (Fig. 7D).
458
459 As many proliferating and cell cycle genes high expressed in 11 RG, rather than 10 RG,
460 we further analysis the cell cycle of cell types. Excitatory neuron exhibited a profile highly
461 similar to interneuron that stay at S states, and 10 RG kept at G1/S states. In contrast, 11
462 RG, 12 G2/M and 13 GE continued cell division (Fig. 7E, F).
463
464
465
466
467
468
469
470
471
472
473
474
475
476
477
478

DISCUSSION

We have systematically analyzed scRNA-seq data to integrate and compare developing human and mouse cerebral cortex, including identified cell type diversities, developing trajectories, gene expression patterns, functional protein association networks, signal transduction pathways and ligand receptor interaction analysis.

According to previous reports, neocortical projection neurons are generated in an "inside-out" fashion by diverse progenitor types in the VZ and SVZ, for example, cut-like homeobox 2-positive (*Cux2*+) progenitors produce the most superficial-layer (upper) [74, 75], which is resided callosal projection neurons (CPN) and high expression marker gene (*SATB2*), whereas corticofugal-layer (deep) neurons derive from Cux2-negative (*Cux2*–) progenitors, which include a large number of corticothalamic projection neurons (CThPN) that reside in layer VI, and subcerebral projection neurons (SCPN) that reside in layer V and express *BCL11B* and *FEZF2* [28]. As the result of the basis of current evidence, a number of different models are produced, In line with a previous report, we detected the 'sequential competence states' model is undesirable in mouse and human [28], because the mouse early developing deep layer (02 EXC deep) expressed an upper layer marker (*SATB2*), a deep layer marker (*BCL11B*), a migratory marker (*TIMA2*) and a transcription factor that is expressed in Layer II–III neurons during their migration and differentiation (*POU3F2*) (Fig. S8B), and human developing trajectories (Fig. 3A), suggesting that there is unreasonable that individual progenitors (*Cux2*–) produce a single neuronal subtype: CThPN at a time [28] (Fig. S8F). More significantly, according to our study, we indicated human and mouse exist two developing models. For human, we observed the reconstructed excitatory neuron trajectory, indicating that the deep and upper layer migrate from SVZ independently (Fig. 3A), whereas the deep layer and upper layer ordering are chaos in mouse developing neocortex trajectory (Fig. 3B), and then, we detected the

506 ligand and receptors have differentially expression in human and mouse (Fig. 4E, S5A, B).

507

508 Additionally, *CUX2* expressed differentially in human and mouse, for example, *CUX2* only
509 expressed in upper layer in human (Fig. S8C), while *Cux2* have expression in maturing
510 mouse deep layer neuron (Fig. S8D), indicating that *Cux2*- positive lineage after
511 generating deep-layer neuronal sub-types change their competence state to express *Cux2*
512 and produce CPN to generate upper-layer. The results may suggest that human is more
513 likely to similar the model "independent lineages" and the model "nested multipotential
514 lineages" is more likely to exist in mouse [28] (Fig. 8A).

515

516 We further summary the divergence and conservation of ligand receptor interaction
517 analysis between human and mouse neocortical projection neurons [46] (Fig. 8B). We
518 predicted the neuron migration and differentiation between SVZ and layers that could
519 potentially be triggered by protein-interactions: *PTN_PTPRZ1* and *MDK_PTPRZ1* [50]
520 (Fig. 8B), meanwhile these expression patterns show high expressed in human SVZ to
521 deep layers and upper layers, and mouse SVZ to deep layers and upper layers, and deep
522 layers to upper layers, which are consistent with our predicted two models: human for
523 "independent lineages" and mouse for "nested multipotential lineages" (Fig. 8B, S8E, F).
524 Then, we observed *NOTCH, EFNA*, *EPHA*, *WNT*, *ACKR* and *CCL* signaling in human
525 deep and upper layer with significant function in the development of synaptic and dendritic
526 cells [53] (Fig. 8B).

527

528 Our data also suggest that cognition-linked genes might form robust groupings according
529 species-specific and cell-type expression profiles. We detected many cognition-relative
530 genes expressed earlier in human than mouse, including *PTPRZ1*, *CNR1*, *PTN*, and
531 *CLSTN2* (Fig. 4A, 5A, B, C, S5A, B), that enriched in cognition, learning and memory and
532 behavior pathways [45, 63, 76] (Fig. 5E, S5F), therefore understanding human cognition

533 development is probably earlier than those of mouse. In conclusion, our single-cell
534 analysis provides an essential resource for future studies directed at understanding the
535 difference developing neocortical trajectories, and excitatory neuron sub-types expression
536 profiles, and cognition-relative genes expression profiles during the early human and
537 mouse brain development.
538
539
540
541
542
543
544
545
546
547
548
549
550
551
552
553
554
555
556
557
558
559

METHODS

Data processing of scRNA-seq from Chromium system

In the early data processing, we applied the processed gene-cell data matrix without poor-quality cells from published study. We used Seurat package (v3.1.2) to process secondary filtration [77]. Only cells that expressed more than 500 genes were considered, only genes expressed in at least 5 single cells were included for further analysis. Additionally, we selected the homologous genes between human and mouse to process further analysis. In total, 12350 genes across 18446 mouse and 6623 human single cells remained for subsequent analysis. The data were normalized to a total of 1×10^4 molecules per cell for the sequencing depth using the Seurat package. The batch effect was mitigated by using the ScaleData function of Seurat (v3.1.2).

Data integration of scRNA-seq and identification of cell types

The Seurat package (v3.1.2) was used to integrate human and mouse scRNA-seq data. We applied the new normalization method 'SCTransform' to process cross-species clustering in order to better operation downstream integration [77]. Then, the Seurat package was used to perform linear dimensional reduction. we used SelectIntegrationFeatures or FindVariableFeatures function from Seurat and further analysis used 'FindIntegrationAnchors' to select 2000 highly variable genes as input for PCA. Then we identified significant PCs based on the JackStrawPlot function. Strong PC1-PC30 were used for UMAP to cluster the cells by FindClusters function with resolution 0.8. Clusters were identified by the expression of known cell-type markers. The markers EOMES, NEUROD6, GAD2 and MKI67 were used to identify the basic cell-type, including progenitor cells, excitatory neurons, inhibitory neurons and astrocytes, respectively.

Identification of DEGs between clusters

587 The DEGs of each cluster were identified using FindAllMarkers function (min.pct = 0,
588 logfc.threshold = 0, test.use = “wilcox”) with the Seurat R package [77]. We used the
589 Wilcoxon rank-sum test (default), and top 10 DE genes ($p < 0.05$) by fold change were
590 identified for each cluster.
591
592 **Correlation Analysis**
593 For correlation analysis of merged human single cell and mouse single cell data, we used
594 integrated data from Seurat package and the Pearson-correlation coefficient calculated in
595 Hmisc package (version 4.3-0), and the relative visualization used package pheatmap
596 (version 1.0.12).
597
598 **Constructing single cell trajectories in cerebral cortex**
599 The Monocle 2 R package (version 2.10.1) were applied to construct single cell pseudo-
600 time trajectories to discover developmental transitions [78]. We used data matrix from
601 Seurat with 2000 highly variable genes into pseudo-time order. we then called
602 ‘differentialGeneTest’ to process DEGs analysis in different cell-types. ‘DDRTree’ were
603 applied to reduce dimensional space and “orderCells” were used to sort cells. The
604 minimum spanning tree on cells and marker genes expression profiles were plotted using
605 the visualization functions “plot_cell_trajectory” for Monocle 2
606
607 **Identifying genes relative to cell fate choices**
608 We analyzed branches in single cell trajectories by BEAM and calILRs function, and we
609 selected genes with q-value < 0.01 and a mean expression value ≥ 0.18, Genes
610 dynamically expressed along the different branches were clustered using the
611 plot_multiple_branches_heatmap function and plot_genes_branched_heatmap function,
612 and Enriched GO terms of cluster-grouped genes were identified using clusterProfiler
613 package (version 3.10.1) [79]. Then, genes were clustered into different clusters by using

614 ‘plot_multiple_branches_pseudotime’ and ‘plot_genes_branched_pseudotime’ to
615 visualize the expression profiles in different cell-types.
616
617 **GO enrichment analysis**
618 Gene ontology (GO) biological process enrichment analysis were performed on differently
619 expressed genes (DEGs) (p-value < 0.05, fold change (FC) > 1) using clusterProfiler
620 package (version 3.10.1) and Metascape [79, 80].
621
622 **Analysing inter-lineage interactions within the neocortex**
623 For comprehensive systematic analysis of inter-lineage interactions within the neocortex,
624 we use CellPhoneDB [46]. We used gene-cell matrix data from Seurat packages after
625 integration as the input data, and we considered only ligands and receptors expressed in
626 greater than 10% of the cells in any given subpopulation. Then, we seted the P-Value 0.05
627 to ensure the prominence. We called ‘cellphonedb plot dot_plot’ to visualize the ligand-
628 receptor interactions within the neocortical projection neuron.
629
630 **Comparing gene expression pattern divergence**
631 The pseudo-time of each cell was assigned by Monocle2, and used median function in R
632 to calculate the mean of pseudo-time in mouse and human trajectories, dividing cells into
633 two categories, including early stage of the cells and the latter stage of cells. and we
634 reconstructed the clustering included 132500 homologous genes within human and
635 mouse by using Seurat package [77, 78]. FindMarkers function helps us to calculate the
636 expression profiles between these two groups, and genes with average expression
637 difference > 0.585 natural log with $P < 0.05$ were selected as DEGs between human and
638 mouse. a part of genes visualized by ‘plot_pseudotime_heatmap’ function.
639
640 **Functional protein association networks analysis**

641 Functional protein association networks were calculated on DEGs using STRING, the
642 results visualized using Cytoscape [72, 81].
643

644 **Connecting transcription factors to target genes**

645 To find the potential transcription factors, TRRUST was used for search transcriptional
646 regulatory interactions [82], and the results visulized using Cytoscape [72, 81].

647

648 **Cell-cycle analysis**

649 In the cell-cycle analysis, we applied scran packge in R (version 1.10.2) to score G1, S
650 and G2/M states of each cells [83]. we selected a cell-cycle related gene set with 43 genes
651 expressed during S and 54 genes expressed during G2/M from Seurat package [77].
652 These gene sets should be anti-correlated in their expression levels, and cells expressing
653 neither are likely to be in the G1 phase (not cycling).
654

655 **Statistical analysis**

656 Comparisons between two groups were made using wilcox. Sample size and P values
657 are given in the Figure legends.

658

659 **ACKNOWLEDGMENTS**

660 This work was supported by the Strategic Priority Research Program of the Chinese
661 Academy of Sciences (Grant No. XDA16010114)
662
663
664
665
666

667 REFERENCES

668

669 1. Otis EM, Brent R: **Equivalent ages in mouse and human embryos.** *The Anatomical record* 1954,
670 **120:**33-63.
671 2. Workman AD, Charvet CJ, Clancy B, Darlington RB, Finlay BL: **Modeling transformations of**
672 **neurodevelopmental sequences across mammalian species.** *Journal of Neuroscience* 2013,
673 **33:**7368-7383.
674 3. Wichterle H, Turnbull DH, Nery S, Fishell G, Alvarez-Buylla A: **In utero fate mapping reveals distinct**
675 **migratory pathways and fates of neurons born in the mammalian basal forebrain.** *Development*
676 2001, **128:**3759-3771.
677 4. Cobos I, Puelles L, Martínez S: **The avian telencephalic subpallium originates inhibitory neurons**
678 **that invade tangentially the pallium (dorsal ventricular ridge and cortical areas).** *Developmental*
679 *biology* 2001, **239:**30-45.
680 5. Wonders CP, Anderson SA: **The origin and specification of cortical interneurons.** *Nature Reviews*
681 *Neuroscience* 2006, **7:**687-696.
682 6. Guo J, Anton E: **Decision making during interneuron migration in the developing cerebral cortex.**
683 *Trends in cell biology* 2014, **24:**342-351.
684 7. Gorski JA, Talley T, Qiu M, Puelles L, Rubenstein JL, Jones KR: **Cortical excitatory neurons and glia,**
685 **but not GABAergic neurons, are produced in the Emx1-expressing lineage.** *Journal of*
686 *Neuroscience* 2002, **22:**6309-6314.
687 8. Molyneaux BJ, Arlotta P, Menezes JR, Macklis JD: **Neuronal subtype specification in the cerebral**
688 **cortex.** *Nature reviews neuroscience* 2007, **8:**427-437.
689 9. Nowakowski TJ, Bhaduri A, Pollen AA, Alvarado B, Mostajo-Radji MA, Di Lullo E, Haeussler M,
690 Sandoval-Espinosa C, Liu SJ, Velmeshev D: **Spatiotemporal gene expression trajectories reveal**
691 **developmental hierarchies of the human cortex.** *Science* 2017, **358:**1318-1323.
692 10. Hodge RD, Bakken TE, Miller JA, Smith KA, Barkan ER, Graybuck LT, Close JL, Long B, Johansen N,
693 Penn O: **Conserved cell types with divergent features in human versus mouse cortex.** *Nature* 2019,
694 **573:**61-68.
695 11. Molnár Z, Métin C, Stoykova A, Tarabykin V, Price DJ, Francis F, Meyer G, Dehay C, Kennedy H:
696 **Comparative aspects of cerebral cortical development.** *European Journal of Neuroscience* 2006,
697 **23:**921-934.
698 12. Monuki ES, Walsh CA: **Mechanisms of cerebral cortical patterning in mice and humans.** *Nature*
699 *neuroscience* 2001, **4:**1199-1206.
700 13. Yuan G-C, Cai L, Elowitz M, Enver T, Fan G, Guo G, Irizarry R, Kharchenko P, Kim J, Orkin S: **Challenges**
701 **and emerging directions in single-cell analysis.** *Genome biology* 2017, **18:**84.
702 14. Poirion OB, Zhu X, Ching T, Garmire L: **Single-cell transcriptomics bioinformatics and**
703 **computational challenges.** *Frontiers in genetics* 2016, **7:**163.
704 15. Papalexi E, Satija R: **Single-cell RNA sequencing to explore immune cell heterogeneity.** *Nature*
705 *Reviews Immunology* 2018, **18:**35.
706 16. Giladi A, Amit I: **Single-cell genomics: a stepping stone for future immunology discoveries.** *Cell*

2018, **172:**14-21.

17. Zhong S, Zhang S, Fan X, Wu Q, Yan L, Dong J, Zhang H, Li L, Sun L, Pan N: **A single-cell RNA-seq survey of the developmental landscape of the human prefrontal cortex.** *Nature* 2018, **555:**524-528.

18. Loo L, Simon JM, Xing L, McCoy ES, Niehaus JK, Guo J, Anton E, Zylka MJ: **Single-cell transcriptomic analysis of mouse neocortical development.** *Nature communications* 2019, **10:**1-11.

19. McInnes L, Healy J, Melville J: **Umap: Uniform manifold approximation and projection for dimension reduction.** *arXiv preprint arXiv:180203426* 2018.

20. Camp JG, Badsha F, Florio M, Kanton S, Gerber T, Wilsch-Bräuninger M, Lewitus E, Sykes A, Hevers W, Lancaster M: **Human cerebral organoids recapitulate gene expression programs of fetal neocortex development.** *Proceedings of the National Academy of Sciences* 2015, **112:**15672-15677.

21. Han X, Wang R, Zhou Y, Fei L, Sun H, Lai S, Saadatpour A, Zhou Z, Chen H, Ye F: **Mapping the mouse cell atlas by microwell-seq.** *Cell* 2018, **172:**1091-1107. e1017.

22. Englund C, Fink A, Lau C, Pham D, Daza RA, Bulfone A, Kowalczyk T, Hevner RF: **Pax6, Tbr2, and Tbr1 are expressed sequentially by radial glia, intermediate progenitor cells, and postmitotic neurons in developing neocortex.** *Journal of Neuroscience* 2005, **25:**247-251.

23. Nagao M, Ogata T, Sawada Y, Gotoh Y: **Zbtb20 promotes astrocytogenesis during neocortical development.** *Nature communications* 2016, **7:**1-14.

24. Nielsen JV, Thomassen M, Møllgård K, Noraberg J, Jensen NA: **Zbtb20 defines a hippocampal neuronal identity through direct repression of genes that control projection neuron development in the isocortex.** *Cerebral Cortex* 2014, **24:**1216-1229.

25. Doeppner TR, Herz J, Bähr M, Tonchev AB, Stoykova A: **Zbtb20 regulates developmental neurogenesis in the olfactory bulb and gliogenesis after adult brain injury.** *Molecular neurobiology* 2019, **56:**567-582.

26. Kohwi M, Petryniak MA, Long JE, Ekker M, Obata K, Yanagawa Y, Rubenstein JL, Alvarez-Buylla A: **A subpopulation of olfactory bulb GABAergic interneurons is derived from Emx1-and Dlx5/6-expressing progenitors.** *Journal of Neuroscience* 2007, **27:**6878-6891.

27. Arnold SJ, Huang G-J, Cheung AF, Era T, Nishikawa S-I, Bikoff EK, Molnár Z, Robertson EJ, Groszer M: **The T-box transcription factor Eomes/Tbr2 regulates neurogenesis in the cortical subventricular zone.** *Genes & development* 2008, **22:**2479-2484.

28. Greig LC, Woodworth MB, Galazo MJ, Padmanabhan H, Macklis JD: **Molecular logic of neocortical projection neuron specification, development and diversity.** *Nature Reviews Neuroscience* 2013, **14:**755-769.

29. Leifer D, Krainc D, Yu Y-T, McDermott J, Breitbart RE, Heng J, Neve RL, Kosofsky B, Nadal-Ginard B, Lipton SA: **MEF2C, a MADS/MEF2-family transcription factor expressed in a laminar distribution in cerebral cortex.** *Proceedings of the National Academy of Sciences* 1993, **90:**1546-1550.

30. Tomita K, Gotoh H, Tomita K, Yamauchi N, Sanbo M: **Multiple patterns of spatiotemporal changes in layer-specific gene expression in the developing visual cortex of higher mammals.** *Neuroscience research* 2012, **73:**207-217.

31. Mayer C, Hafemeister C, Bandler RC, Machold R, Brito RB, Jaglin X, Allaway K, Butler A, Fishell G, Satija R: **Developmental diversification of cortical inhibitory interneurons.** *Nature* 2018, **555:**457-

748 462.
749 32. Tasic B, Menon V, Nguyen TN, Kim TK, Jarsky T, Yao Z, Levi B, Gray LT, Sorensen SA, Dolbeare T: **Adult**
750 **mouse cortical cell taxonomy revealed by single cell transcriptomics.** *Nature neuroscience* 2016,
751 **19:**335.
752 33. Mi D, Li Z, Lim L, Li M, Moissidis M, Yang Y, Gao T, Hu TX, Pratt T, Price DJ: **Early emergence of**
753 **cortical interneuron diversity in the mouse embryo.** *Science* 2018, **360:**81-85.
754 34. Ghanem N, Yu M, Long J, Hatch G, Rubenstein JL, Ekker M: **Distinct cis-regulatory elements from**
755 **the Dlx1/Dlx2 locus mark different progenitor cell populations in the ganglionic eminences and**
756 **different subtypes of adult cortical interneurons.** *Journal of Neuroscience* 2007, **27:**5012-5022.
757 35. Donovan SL, Mamounas LA, Andrews AM, Blue ME, McCasland JS: **GAP-43 is critical for normal**
758 **development of the serotonergic innervation in forebrain.** *Journal of Neuroscience* 2002, **22:**3543-
759 3552.
760 36. Desplats PA, Lambert JR, Thomas EA: **Functional roles for the striatal-enriched transcription factor,**
761 **Bcl11b, in the control of striatal gene expression and transcriptional dysregulation in**
762 **Huntington's disease.** *Neurobiology of disease* 2008, **31:**298-308.
763 37. Geirsdottir L, David E, Keren-Shaul H, Weiner A, Bohlen SC, Neuber J, Balic A, Giladi A, Sheban F,
764 Dutertre C-A: **Cross-Species Single-Cell Analysis Reveals Divergence of the Primate Microglia**
765 **Program.** *Cell* 2019, **179:**1609-1622. e1616.
766 38. Jansen IE, Savage JE, Watanabe K, Bryois J, Williams DM, Steinberg S, Sealock J, Karlsson IK, Hägg S,
767 Athanasiu L: **Genome-wide meta-analysis identifies new loci and functional pathways influencing**
768 **Alzheimer's disease risk.** *Nature genetics* 2019, **51:**404-413.
769 39. Lambert J, Ibrahim-Verbaas C, Harold D, Naj A, Sims R, Bellenguez C, DeStafano A, Bis J, Beecham
770 G, Grenier-Boley B: **European Alzheimer's Disease Initiative (EADI); Genetic and Environmental**
771 **Risk in Alzheimer's Disease; Alzheimer's Disease Genetic Consortium; Cohorts for Heart and**
772 **Aging Research in Genomic Epidemiology. Meta-analysis of 74,046 individuals identifies 11 new**
773 **susceptibility loci for Alzheimer's disease.** *Nat Genet* 2013, **45:**1452-1458.
774 40. Keren-Shaul H, Spinrad A, Weiner A, Matcovitch-Natan O, Dvir-Szternfeld R, Ulland TK, David E,
775 Baruch K, Lara-Astaiso D, Toth B: **A unique microglia type associated with restricting development**
776 **of Alzheimer's disease.** *Cell* 2017, **169:**1276-1290. e1217.
777 41. Lim DA, Alvarez-Buylla A: **The adult ventricular–subventricular zone (V-SVZ) and olfactory bulb**
778 **(OB) neurogenesis.** *Cold Spring Harbor perspectives in biology* 2016, **8:**a018820.
779 42. Wang T-W, Zhang H, Parent JM: **Retinoic acid regulates postnatal neurogenesis in the murine**
780 **subventricular zone-olfactory bulb pathway.** *Development* 2005, **132:**2721-2732.
781 43. O'rourke NA, Weiler NC, Micheva KD, Smith SJ: **Deep molecular diversity of mammalian synapses:**
782 **why it matters and how to measure it.** *Nature Reviews Neuroscience* 2012, **13:**365-379.
783 44. Fantin A, Maden CH, Ruhrberg C: **Neuropilin ligands in vascular and neuronal patterning.** Portland
784 Press Ltd.; 2009.
785 45. Lipina TV, Prasad T, Yokomaku D, Luo L, Connor SA, Kawabe H, Wang YT, Brose N, Roder JC, Craig
786 AM: **Cognitive deficits in calsyntenin-2-deficient mice associated with reduced GABAergic**
787 **transmission.** *Neuropsychopharmacology* 2016, **41:**802.
788 46. Efremova M, Vento-Tormo M, Teichmann SA, Vento-Tormo R: **CellPhoneDB v2. 0: Inferring cell-cell**

communication from combined expression of multi-subunit receptor-ligand complexes. *bioRxiv* 2019**:**680926.

47. Janoueix-Lerosey I, Lopez-Delisle L, Delattre O, Rohrer H: **The ALK receptor in sympathetic neuron development and neuroblastoma.** *Cell and tissue research* 2018, **372:**325-337.

48. Motegi A, Fujimoto J, Kotani M, Sakuraba H, Yamamoto T: **ALK receptor tyrosine kinase promotes cell growth and neurite outgrowth.** *Journal of cell science* 2004, **117:**3319-3329.

49. Wellstein A: **ALK receptor activation, ligands and therapeutic targeting in glioblastoma and in other cancers.** *Frontiers in oncology* 2012, **2:**192.

50. Herradon G, Pérez‐García C: **Targeting midkine and pleiotrophin signalling pathways in addiction and neurodegenerative disorders: recent progress and perspectives.** *British journal of pharmacology* 2014, **171:**837-848.

51. Rusanescu G, Mao J: **Notch3 is necessary for neuronal differentiation and maturation in the adult spinal cord.** *Journal of cellular and molecular medicine* 2014, **18:**2103-2116.

52. Dvoriantchikova G, Perea-Martinez I, Pappas S, Barry AF, Danek D, Dvoriantchikova X, Pelaez D, Ivanov D: **Molecular characterization of notch1 positive progenitor cells in the developing retina.** *PloS one* 2015, **10**.

53. Palmer A, Klein R: **Multiple roles of ephrins in morphogenesis, neuronal networking, and brain function.** *Genes & development* 2003, **17:**1429-1450.

54. Yuferov V, Ho A, Morgello S, Yang Y, Ott J, Kreek MJ: **Expression of ephrin receptors and ligands in postmortem brains of HIV-infected subjects with and without cognitive impairment.** *Journal of Neuroimmune Pharmacology* 2013, **8:**333-344.

55. Paganoni S, Bernstein J, Ferreira A: **Ror1-Ror2 complexes modulate synapse formation in hippocampal neurons.** *Neuroscience* 2010, **165:**1261-1274.

56. Hansell CA, MacLellan LM, Oldham RS, Doonan J, Chapple KJ, Anderson EJ, Linington C, McInnes IB, Nibbs RJ, Goodyear CS: **The atypical chemokine receptor ACKR2 suppresses Th17 responses to protein autoantigens.** *Immunology and cell biology* 2015, **93:**167-176.

57. Harkany T, Keimpema E, Barabás K, Mulder J: **Endocannabinoid functions controlling neuronal specification during brain development.** *Molecular and cellular endocrinology* 2008, **286:**S84-S90.

58. Mulder J, Aguado T, Keimpema E, Barabás K, Rosado CJB, Nguyen L, Monory K, Marsicano G, Di Marzo V, Hurd YL: **Endocannabinoid signaling controls pyramidal cell specification and long-range axon patterning.** *Proceedings of the National Academy of Sciences* 2008, **105:**8760-8765.

59. Watson S, Chambers D, Hobbs C, Doherty P, Graham A: **The endocannabinoid receptor, CB1, is required for normal axonal growth and fasciculation.** *Molecular and Cellular Neuroscience* 2008, **38:**89-97.

60. Wu CS, Zhu J, Wager‐Miller J, Wang S, O'Leary D, Monory K, Lutz B, Mackie K, Lu HC: **Requirement of cannabinoid CB1 receptors in cortical pyramidal neurons for appropriate development of corticothalamic and thalamocortical projections.** *European Journal of Neuroscience* 2010, **32:**693-706.

61. Keimpema E, Barabas K, Morozov YM, Tortoriello G, Torii M, Cameron G, Yanagawa Y, Watanabe M, Mackie K, Harkany T: **Differential subcellular recruitment of monoacylglycerol lipase generates spatial specificity of 2-arachidonoyl glycerol signaling during axonal pathfinding.** *Journal of*

830 *Neuroscience* 2010, **30:**13992-14007.
831 62. Mackie K: **Signaling via CNS cannabinoid receptors.** *Molecular and cellular endocrinology* 2008,
832 **286:**S60-S65.
833 63. Bilkei-Gorzo A, Racz I, Valverde O, Otto M, Michel K, Sarstre M, Zimmer A: **Early age-related**
834 **cognitive impairment in mice lacking cannabinoid CB1 receptors.** *Proceedings of the National*
835 *Academy of Sciences* 2005, **102:**15670-15675.
836 64. Schneider M, Kasanetz F, Lynch DL, Friemel CM, Lassalle O, Hurst DP, Steindel F, Monory K, Schäfer
837 C, Miederer I: **Enhanced functional activity of the cannabinoid type-1 receptor mediates**
838 **adolescent behavior.** *Journal of Neuroscience* 2015, **35:**13975-13988.
839 65. Juhász G, Csepany E, Magyar M, Édes AE, Eszlári N, Hullam G, Antal P, Kokonyei G, Anderson I,
840 Deakin J: **Variants in the CNR1 gene predispose to headache with nausea in the presence of life**
841 **stress.** *Genes, Brain and Behavior* 2017, **16:**384-393.
842 66. Jandrig B, Seitz S, Hinzmann B, Arnold W, Micheel B, Koelble K, Siebert R, Schwartz A, Ruecker K,
843 Schlag PM: **ST18 is a breast cancer tumor suppressor gene at human chromosome 8q11. 2.**
844 *Oncogene* 2004, **23:**9295-9302.
845 67. Raivich G, Bohatschek M, Da Costa C, Iwata O, Galiano M, Hristova M, Nateri AS, Makwana M,
846 Riera-Sans Ls, Wolfer DP: **The AP-1 transcription factor c-Jun is required for efficient axonal**
847 **regeneration.** *Neuron* 2004, **43:**57-67.
848 68. Yamasaki T, Kawasaki H, Nishina H: **Diverse roles of JNK and MKK pathways in the brain.** *Journal*
849 *of signal transduction* 2012, **2012**.
850 69. Tang C, Wang M, Wang P, Wang L, Wu Q, Guo W: **Neural stem cells behave as a functional niche**
851 **for the maturation of newborn neurons through the secretion of PTN.** *Neuron* 2019, **101:**32-44.
852 e36.
853 70. González-Castillo C, Ortuño-Sahagún D, Guzmán-Brambila C, Pallàs M, Rojas-Mayorquín AE:
854 **Pleiotrophin as a central nervous system neuromodulator, evidences from the hippocampus.**
855 *Frontiers in cellular neuroscience* 2015, **8:**443.
856 71. Lu KV, Jong KA, Kim GY, Singh J, Dia EQ, Yoshimoto K, Wang MY, Cloughesy TF, Nelson SF, Mischel
857 PS: **Differential induction of glioblastoma migration and growth by two forms of pleiotrophin.**
858 *Journal of Biological Chemistry* 2005, **280:**26953-26964.
859 72. Szklarczyk D, Gable AL, Lyon D, Junge A, Wyder S, Huerta-Cepas J, Simonovic M, Doncheva NT,
860 Morris JH, Bork P: **STRING v11: protein–protein association networks with increased coverage,**
861 **supporting functional discovery in genome-wide experimental datasets.** *Nucleic acids research*
862 2019, **47:**D607-D613.
863 73. Castiglioni V, Faedo A, Onorati M, Bocchi VD, Li Z, Iennaco R, Vuono R, Bulfamante GP, Muzio L,
864 Martino G: **Dynamic and cell-specific DACH1 expression in human neocortical and striatal**
865 **development.** *Cerebral Cortex* 2019, **29:**2115-2124.
866 74. Zimmer C, Tiveron M-C, Bodmer R, Cremer H: **Dynamics of Cux2 expression suggests that an early**
867 **pool of SVZ precursors is fated to become upper cortical layer neurons.** *Cerebral cortex* 2004,
868 **14:**1408-1420.
869 75. Cubelos B, Sebastián-Serrano A, Beccari L, Calcagnotto ME, Cisneros E, Kim S, Dopazo A, Alvarez-
870 Dolado M, Redondo JM, Bovolenta P: **Cux1 and Cux2 regulate dendritic branching, spine**

871 **morphology, and synapses of the upper layer neurons of the cortex.** *Neuron* 2010, **66:**523-535.
872 76. Krellman JW, Ruiz HH, Marciano VA, Mondrow B, Croll SD: **Behavioral and neuroanatomical**
873 **abnormalities in pleiotrophin knockout mice.** *PloS one* 2014, **9**.
874 77. Stuart T, Butler A, Hoffman P, Hafemeister C, Papalexi E, Mauck III WM, Hao Y, Stoeckius M, Smibert
875 P, Satija R: **Comprehensive integration of single-cell data.** *Cell* 2019, **177:**1888-1902. e1821.
876 78. Trapnell C, Cacchiarelli D, Grimsby J, Pokharel P, Li S, Morse M, Lennon NJ, Livak KJ, Mikkelsen TS,
877 Rinn JL: **The dynamics and regulators of cell fate decisions are revealed by pseudotemporal**
878 **ordering of single cells.** *Nature biotechnology* 2014, **32:**381.
879 79. Yu G, Wang L-G, Han Y, He Q-Y: **clusterProfiler: an R package for comparing biological themes**
880 **among gene clusters.** *Omics: a journal of integrative biology* 2012, **16:**284-287.
881 80. Zhou Y, Zhou B, Pache L, Chang M, Khodabakhshi AH, Tanaseichuk O, Benner C, Chanda SK:
882 **Metascape provides a biologist-oriented resource for the analysis of systems-level datasets.**
883 *Nature communications* 2019, **10:**1-10.
884 81. Shannon P, Markiel A, Ozier O, Baliga NS, Wang JT, Ramage D, Amin N, Schwikowski B, Ideker T:
885 **Cytoscape: a software environment for integrated models of biomolecular interaction networks.**
886 *Genome research* 2003, **13:**2498-2504.
887 82. Han H, Cho J-W, Lee S, Yun A, Kim H, Bae D, Yang S, Kim CY, Lee M, Kim E: **TRRUST v2: an expanded**
888 **reference database of human and mouse transcriptional regulatory interactions.** *Nucleic acids*
889 *research* 2018, **46:**D380-D386.
890 83. Lun AT, McCarthy DJ, Marioni JC: **A step-by-step workflow for low-level analysis of single-cell RNA-**
891 **seq data with Bioconductor.** *F1000Research* 2016, **5**.

892

Figure 1

A

Species	Age	Cells	Tissue	Gene number	Reference
Mouse	E14.5 and P0	18,446/18446	Cerebral cortex	13,250	
Human	5.85 to 37 pcw	6,655/6623	Cerebral cortex	13,250	

Species	Age	Cells	Tissue	Gene number	Reference
Mouse	E14.5 and P0	6,655/6655	Cerebral cortex	13,250	
Human	5.85 to 37 pcw	6,655/6623	Cerebral cortex	13,250	

B

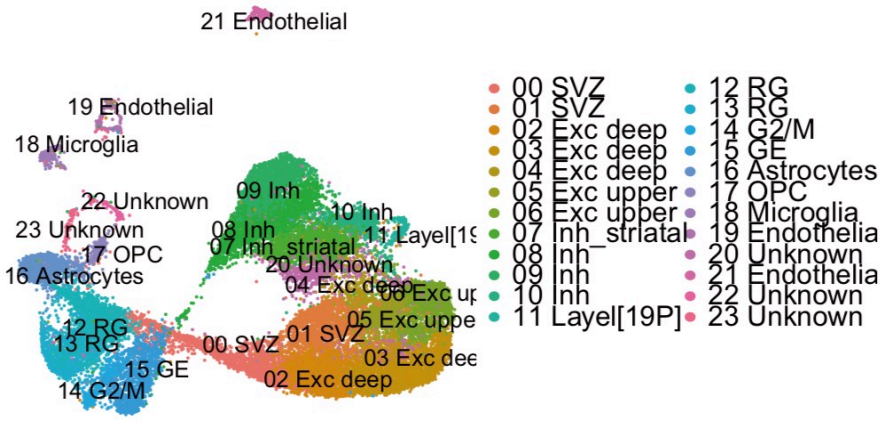

C

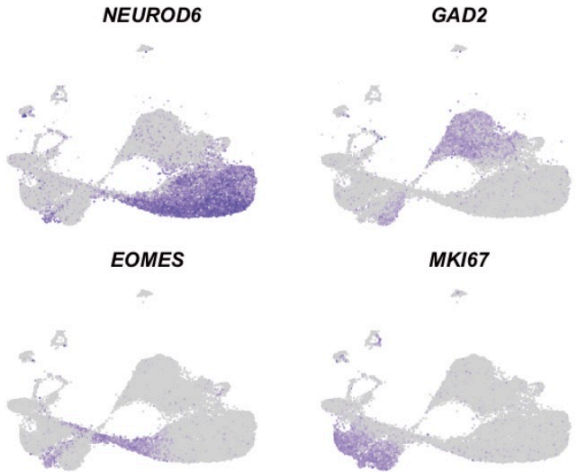

D

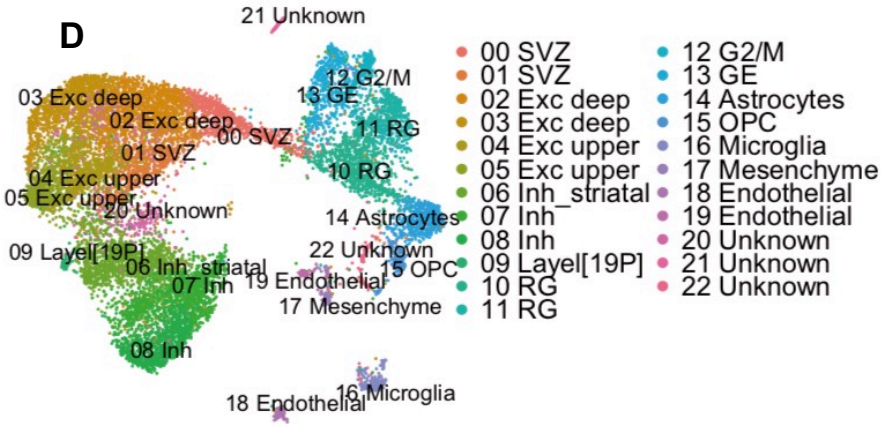

E

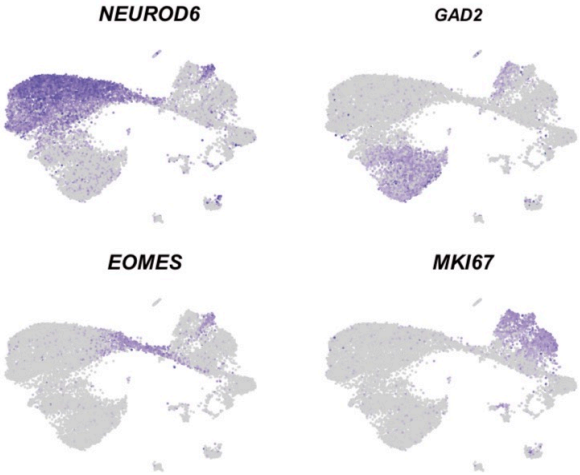

F

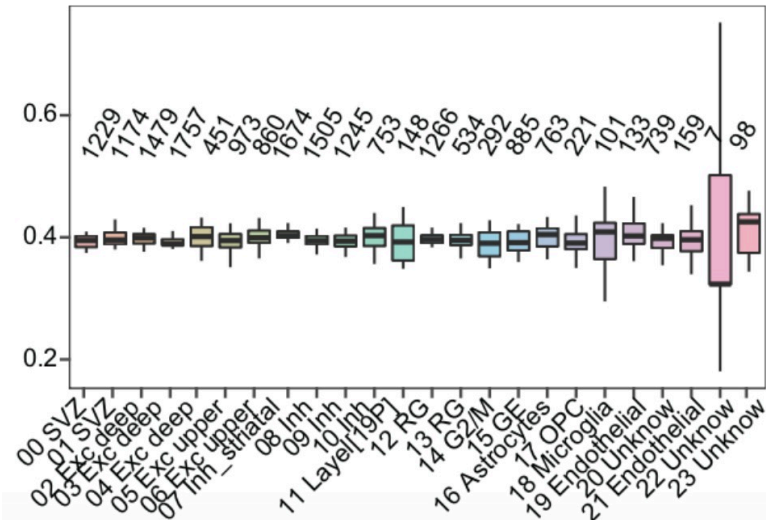

Figure 2

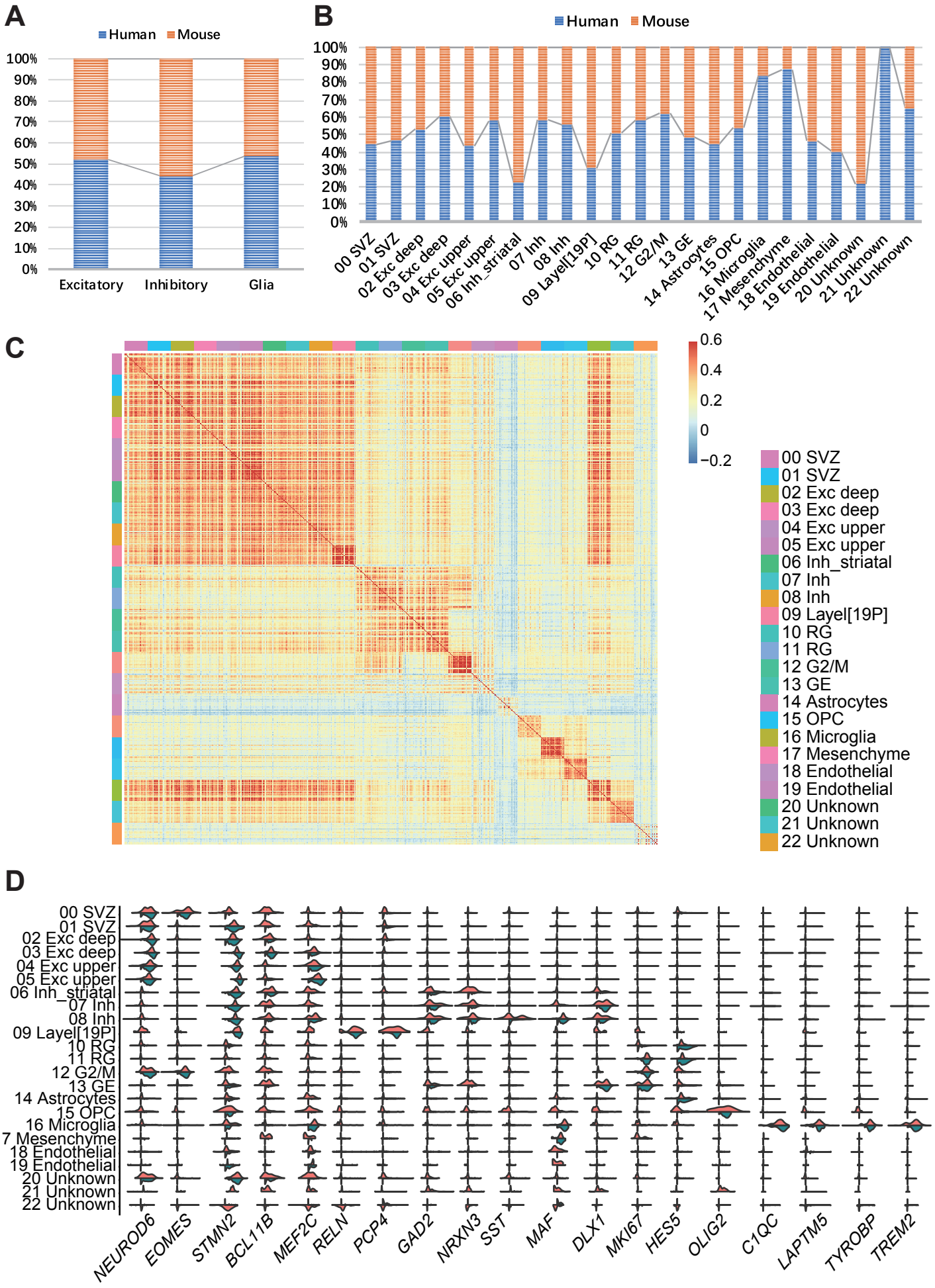
A
Human
Mouse
100%
90%
80%
70%
60%
50%
40%
30%
20%
10%
0%
Excitatory
Inhibitory
Glia
B
Human
Mouse
00 SVZ
01 SVZ
02 Exc deep
03 Exc deep
04 Exc upper
05 Exc upper
06 Inh_striatal
07 Inh
08 Inh
09 Layel[19P]
10 RG
11 RG
12 G2/M
13 GE
14 Astrocytes
15 OPC
16 Microglia
17 Mesenchyme
18 Endothelial
19 Endothelial
20 Unknown
21 Unknown
22 Unknown
C
0.6
0.4
0.2
0
−0.2
00 SVZ
01 SVZ
02 Exc deep
03 Exc deep
04 Exc upper
05 Exc upper
06 Inh_striatal
07 Inh
08 Inh
09 Layel[19P]
10 RG
11 RG
12 G2/M
13 GE
14 Astrocytes
15 OPC
16 Microglia
17 Mesenchyme
18 Endothelial
19 Endothelial
20 Unknown
21 Unknown
22 Unknown
D
NEUROD6
EOMES
STMN2
BCL11B
MEF2C
RELN
PCP4
GAD2
NRXN3
SST
MAF
DLX1
MKI67
HES5
OLIG2
C1QC
LAPTM5
TYROBP
TREM2

Figure 3

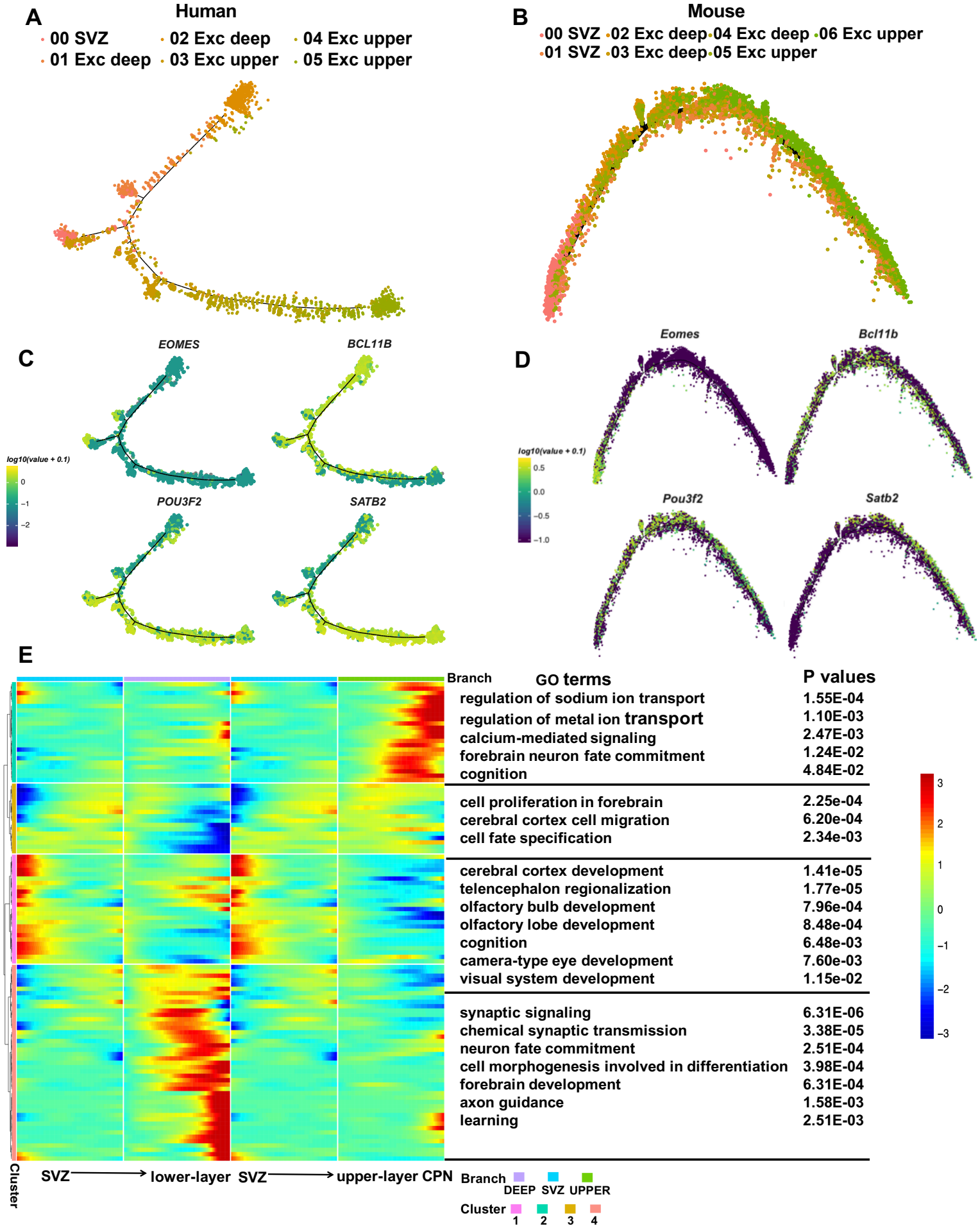
A
Human
00 SVZ
01 Exc deep
02 Exc deep
03 Exc upper
04 Exc upper
05 Exc upper
B
Mouse
00 SVZ
01 SVZ
02 Exc deep
03 Exc deep
04 Exc deep
05 Exc upper
06 Exc upper
C
EOMES
BCL11B
POU3F2
SATB2
log10(value + 0.1)
D
Eomes
Bcl11b
Pou3f2
Satb2
log10(value + 0.1)
E
Branch
GO terms
P values
regulation of sodium ion transport 1.55E-04
regulation of metal ion transport 1.10E-03
calcium-mediated signaling 2.47E-03
forebrain neuron fate commitment 1.24E-02
cognition 4.84E-02
cell proliferation in forebrain 2.25e-04
cerebral cortex cell migration 6.20e-04
cell fate specification 2.34e-03
cerebral cortex development 1.41e-05
telencephalon regionalization 1.77e-05
olfactory bulb development 7.96e-04
olfactory lobe development 8.48e-04
cognition 6.48e-03
camera-type eye development 7.60e-03
visual system development 1.15e-02
synaptic signaling 6.31E-06
chemical synaptic transmission 3.38E-05
neuron fate commitment 2.51E-04
cell morphogenesis involved in differentiation 3.98E-04
forebrain development 6.31E-04
axon guidance 1.58E-03
learning 2.51E-03
Cluster
SVZ → lower-layer SVZ → upper-layer CPN
Branch
DEEP SVZ UPPER
Cluster
1 2 3 4

Figure 4

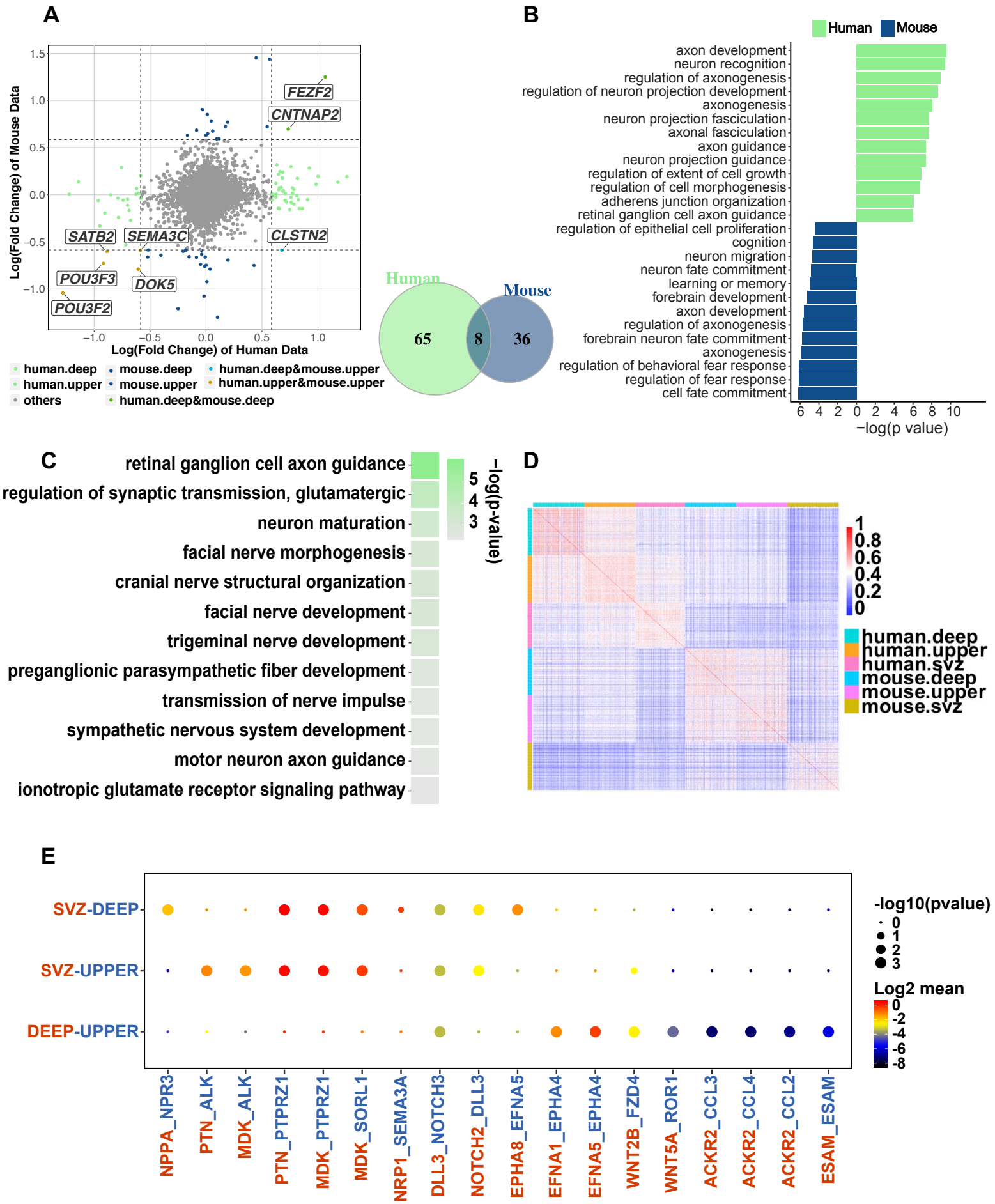
A
Log(Fold Change) of Mouse Data
Log(Fold Change) of Human Data
FEZF2
CNTNAP2
SATB2
SEMA3C
CLSTN2
POU3F3
DOK5
POU3F2
human.deep
human.upper
others
mouse.deep
mouse.upper
human.deep&mouse.deep
human.deep&mouse.upper
human.upper&mouse.upper
Human
Mouse
65
8
36
B
Human
Mouse
axon development
neuron recognition
regulation of axonogenesis
regulation of neuron projection development
axonogenesis
neuron projection fasciculation
axonal fasciculation
axon guidance
neuron projection guidance
regulation of extent of cell growth
regulation of cell morphogenesis
adherens junction organization
retinal ganglion cell axon guidance
regulation of epithelial cell proliferation
cognition
neuron migration
neuron fate commitment
learning or memory
forebrain development
axon development
regulation of axonogenesis
forebrain neuron fate commitment
axonogenesis
regulation of behavioral fear response
regulation of fear response
cell fate commitment
−log(p value)
C
retinal ganglion cell axon guidance
regulation of synaptic transmission, glutamatergic
neuron maturation
facial nerve morphogenesis
cranial nerve structural organization
facial nerve development
trigeminal nerve development
preganglionic parasympathetic fiber development
transmission of nerve impulse
sympathetic nervous system development
motor neuron axon guidance
ionotropic glutamate receptor signaling pathway
−log(p-value)
D
human.deep
human.upper
human.svz
mouse.deep
mouse.upper
mouse.svz
E
SVZ-DEEP
SVZ-UPPER
DEEP-UPPER
NPPA_NPR3
PTN_ALK
MDK_ALK
PTN_PTPRZ1
MDK_PTPRZ1
MDK_SORL1
NRP1_SEMA3A
DLL3_NOTCH3
NOTCH2_DLL3
EPHA8_EFNA5
EFNA1_EPHA4
EFNA5_EPHA4
WNT2B_FZD4
WNT5A_ROR1
ACKR2_CCL3
ACKR2_CCL4
ACKR2_CCL2
ESAM_ESAM
-log10(pvalue)
Log2 mean

Figure 5

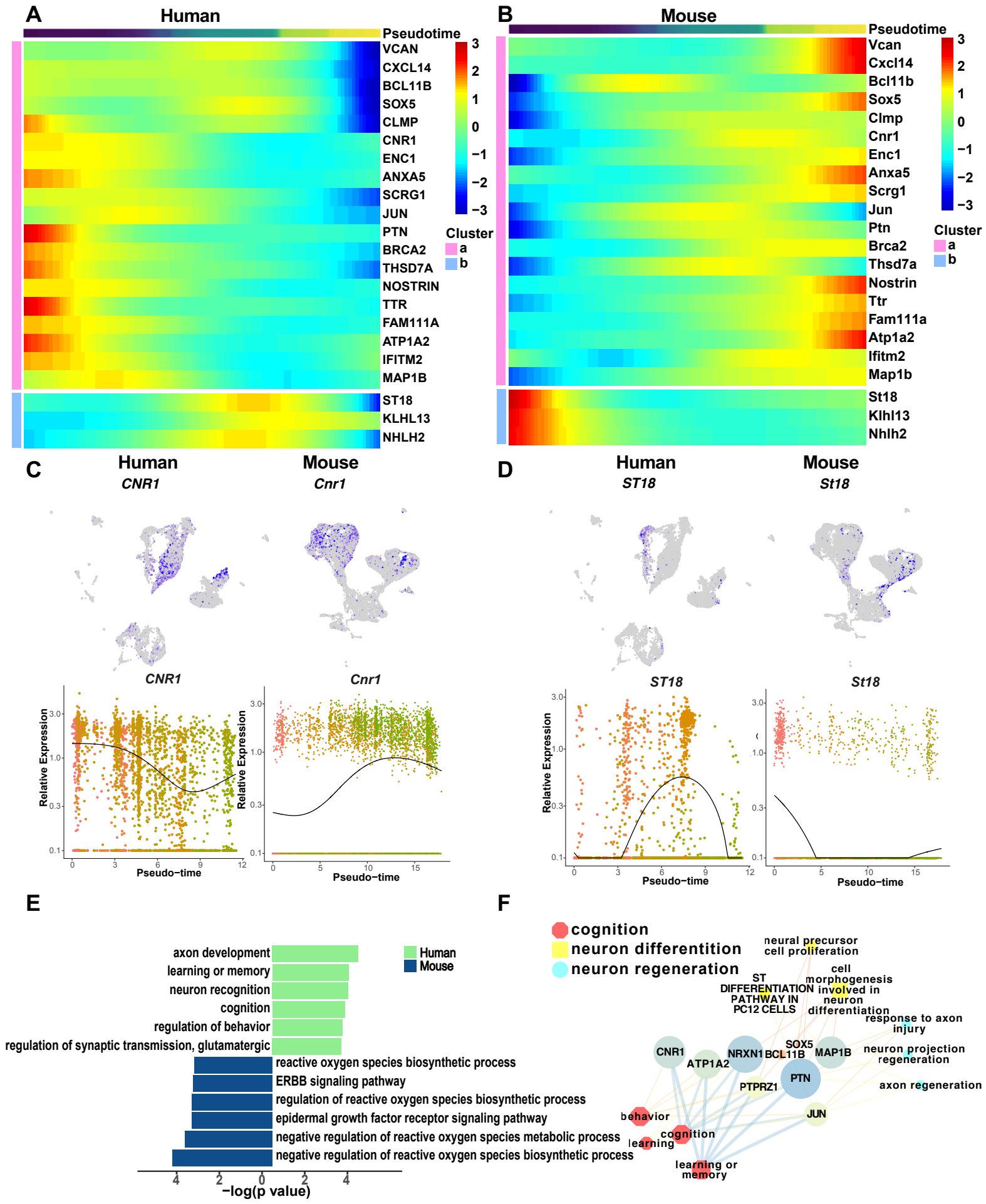
A
Human
Pseudotime
VCAN
CXCL14
BCL11B
SOX5
CLMP
CNR1
ENC1
ANXA5
SCRG1
JUN
PTN
BRCA2
THSD7A
NOSTRIN
TTR
FAM111A
ATP1A2
IFITM2
MAP1B
ST18
KLHL13
NHLH2
Cluster
a
b
B
Mouse
Pseudotime
Vcan
Cxcl14
Bcl11b
Sox5
Clmp
Cnr1
Enc1
Anxa5
Scrg1
Jun
Ptn
Brca2
Thsd7a
Nostrin
Ttr
Fam111a
Atp1a2
Ifitm2
Map1b
St18
Klhl13
Nhlh2
C
Human
CNR1
Mouse
Cnr1
Relative Expression
Pseudo−time
D
Human
ST18
Mouse
St18
E
axon development
learning or memory
neuron recognition
cognition
regulation of behavior
regulation of synaptic transmission, glutamatergic
reactive oxygen species biosynthetic process
ERBB signaling pathway
regulation of reactive oxygen species biosynthetic process
epidermal growth factor receptor signaling pathway
negative regulation of reactive oxygen species metabolic process
negative regulation of reactive oxygen species biosynthetic process
Human
Mouse
−log(p value)
F
cognition
neuron differentition
neuron regeneration
neural precursor cell proliferation
ST DIFFERENTIATION PATHWAY IN PC12 CELLS
cell morphogenesis involved in neuron differentiation
response to axon injury
neuron projection regeneration
axon regeneration
CNR1
ATP1A2
NRXN1
SOX5
BCL11B
MAP1B
PTPRZ1
PTN
JUN
behavior
cognition
learning
learning or memory

Figure 6

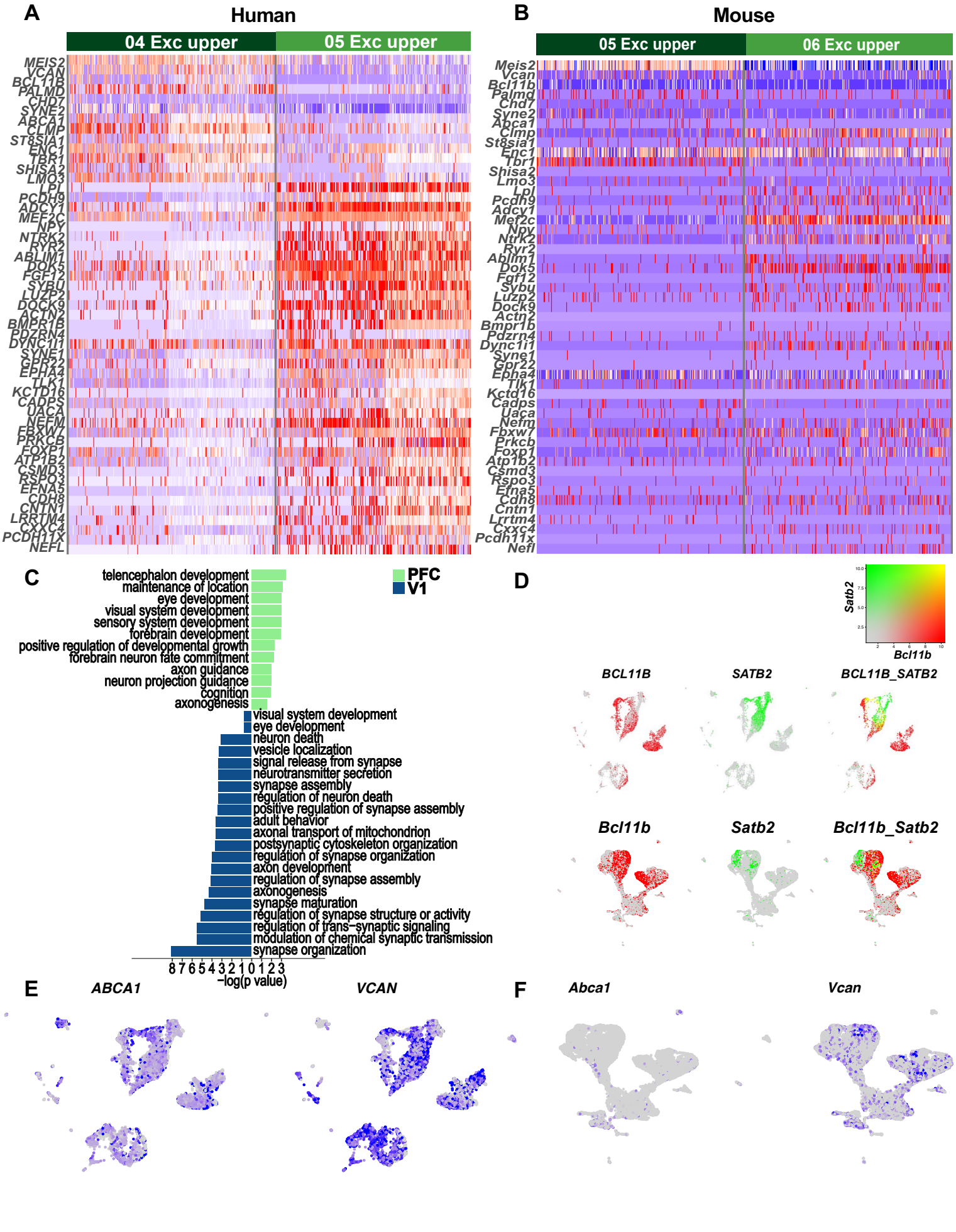
A
Human
04 Exc upper
05 Exc upper
MEIS2
VCAN
BCL11B
PALMD
CHD7
SYNE2
ABCA1
CLMP
ST8SIA1
ENC1
TBR1
SHISA2
LMO3
LPL
PCDH9
ADCY1
MEF2C
NPY
NTRK2
RYR2
ABLIM1
DOK5
FGF12
SYBU
LUZP2
DOCK9
ACTN2
BMPR1B
PDZRN4
DYNC1I1
SYNE1
GPR22
EPHA4
TLK1
KCTD16
CADPS
UACA
NEFM
FBXW7
PRKCB
FOXP1
ATP1B2
CSMD3
RSPO3
EFNA5
CDH8
CNTN1
LRRTM4
CXXC4
PCDH11X
NEFL
B
Mouse
05 Exc upper
06 Exc upper
Meis2
Vcan
Bcl11b
Palmd
Chd7
Syne2
Abca1
Clmp
St8sia1
Enc1
Tbr1
Shisa2
Lmo3
Lpl
Pcdh9
Adcy1
Mef2c
Npy
Ntrk2
Ryr2
Ablim1
Dok5
Fgf12
Sybu
Luzp2
Dock9
Actn2
Bmpr1b
Pdzrn4
Dync1i1
Syne1
Gpr22
Epha4
Tlk1
Kctd16
Cadps
Uaca
Nefm
Fbxw7
Prkcb
Foxp1
Atp1b2
Csmd3
Rspo3
Efna5
Cdh8
Cntn1
Lrrtm4
Cxxc4
Pcdh11x
Nefl
C
PFC
V1
telencephalon development
maintenance of location
eye development
visual system development
sensory system development
forebrain development
positive regulation of developmental growth
forebrain neuron fate commitment
axon guidance
neuron projection guidance
cognition
axonogenesis
visual system development
eye development
neuron death
vesicle localization
signal release from synapse
neurotransmitter secretion
synapse assembly
regulation of neuron death
positive regulation of synapse assembly
adult behavior
axonal transport of mitochondrion
postsynaptic cytoskeleton organization
regulation of synapse organization
axon development
regulation of synapse assembly
axonogenesis
synapse maturation
regulation of synapse structure or activity
regulation of trans-synaptic signaling
modulation of chemical synaptic transmission
synapse organization
8 7 6 5 4 3 2 1 0 1 2 3
−log(p value)
D
Satb2
Bcl11b
BCL11B
SATB2
BCL11B_SATB2
Bcl11b
Satb2
Bcl11b_Satb2
E
ABCA1
VCAN
F
Abca1
Vcan

Figure 7

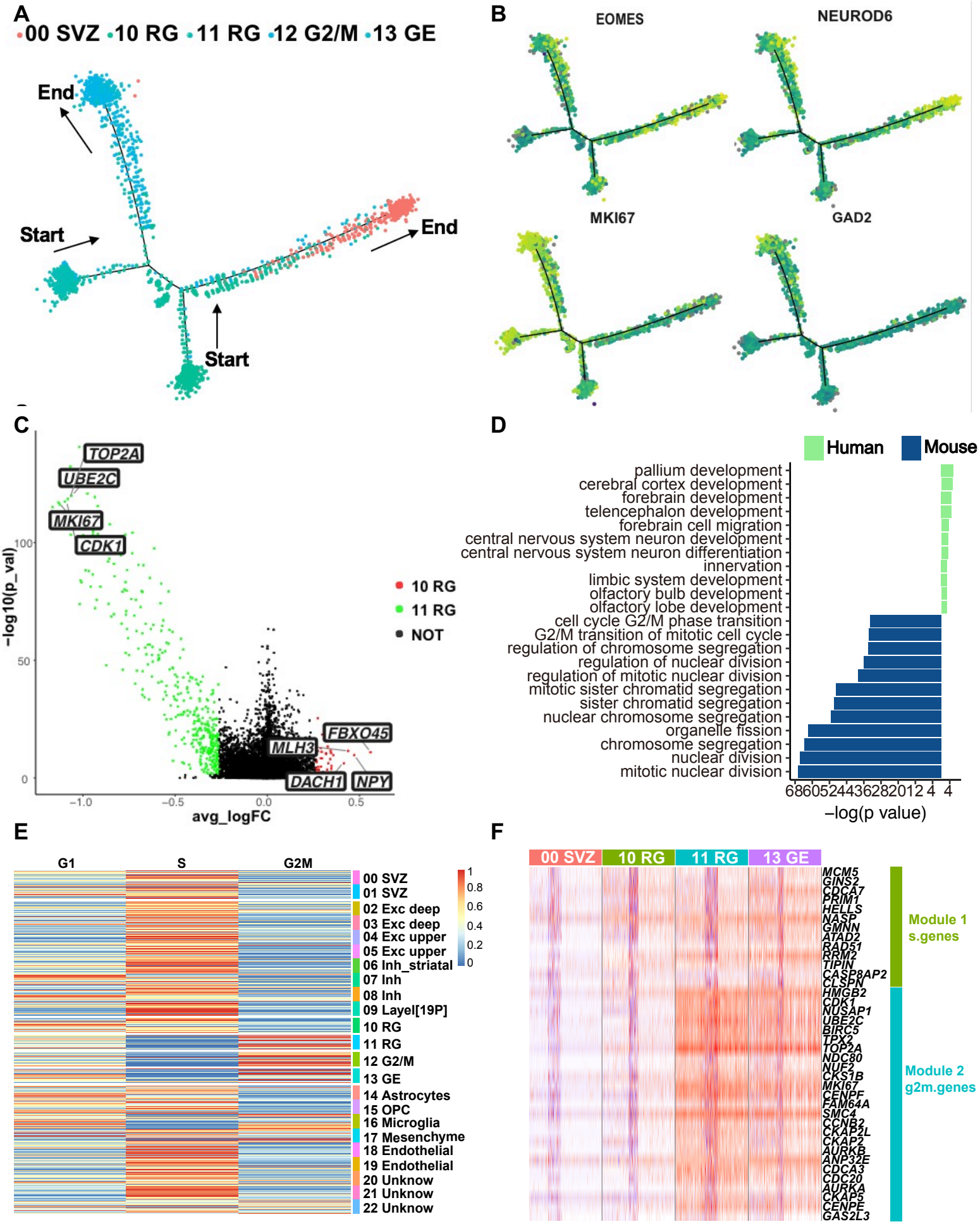
A
00 SVZ
10 RG
11 RG
12 G2/M
13 GE
End
Start
End
Start
B
EOMES
NEUROD6
MKI67
GAD2
C
TOP2A
UBE2C
MKI67
CDK1
FBXO45
MLH3
DACH1
NPY
10 RG
11 RG
NOT
−log10(p_val)
avg_logFC
D
Human
Mouse
pallium development
cerebral cortex development
forebrain development
telencephalon development
forebrain cell migration
central nervous system neuron development
central nervous system neuron differentiation
innervation
limbic system development
olfactory bulb development
olfactory lobe development
cell cycle G2/M phase transition
G2/M transition of mitotic cell cycle
regulation of chromosome segregation
regulation of nuclear division
regulation of mitotic nuclear division
mitotic sister chromatid segregation
sister chromatid segregation
nuclear chromosome segregation
organelle fission
chromosome segregation
nuclear division
mitotic nuclear division
–log(p value)
E
G1
S
G2M
00 SVZ
01 SVZ
02 Exc deep
03 Exc deep
04 Exc upper
05 Exc upper
06 Inh_striatal
07 Inh
08 Inh
09 Layel[19P]
10 RG
11 RG
12 G2/M
13 GE
14 Astrocytes
15 OPC
16 Microglia
17 Mesenchyme
18 Endothelial
19 Endothelial
20 Unknow
21 Unknow
22 Unknow
F
00 SVZ
10 RG
11 RG
13 GE
MCM5
GINS2
CDCA7
PRIM1
HELLS
NASP
GMNN
ATAD2
RAD51
RRM2
TIPIN
CASP8AP2
CLSPN
HMGB2
CDK1
NUSAP1
UBE2C
BIRC5
TPX2
TOP2A
NDC80
NUF2
CKS1B
MKI67
CENPF
FAM64A
SMC4
CCNB2
CKAP2L
CKAP2
AURKB
ANP32E
CDCA3
CDC20
AURKA
CKAP5
CENPE
GAS2L3
Module 1
s.genes
Module 2
g2m.genes

Figure 8

A

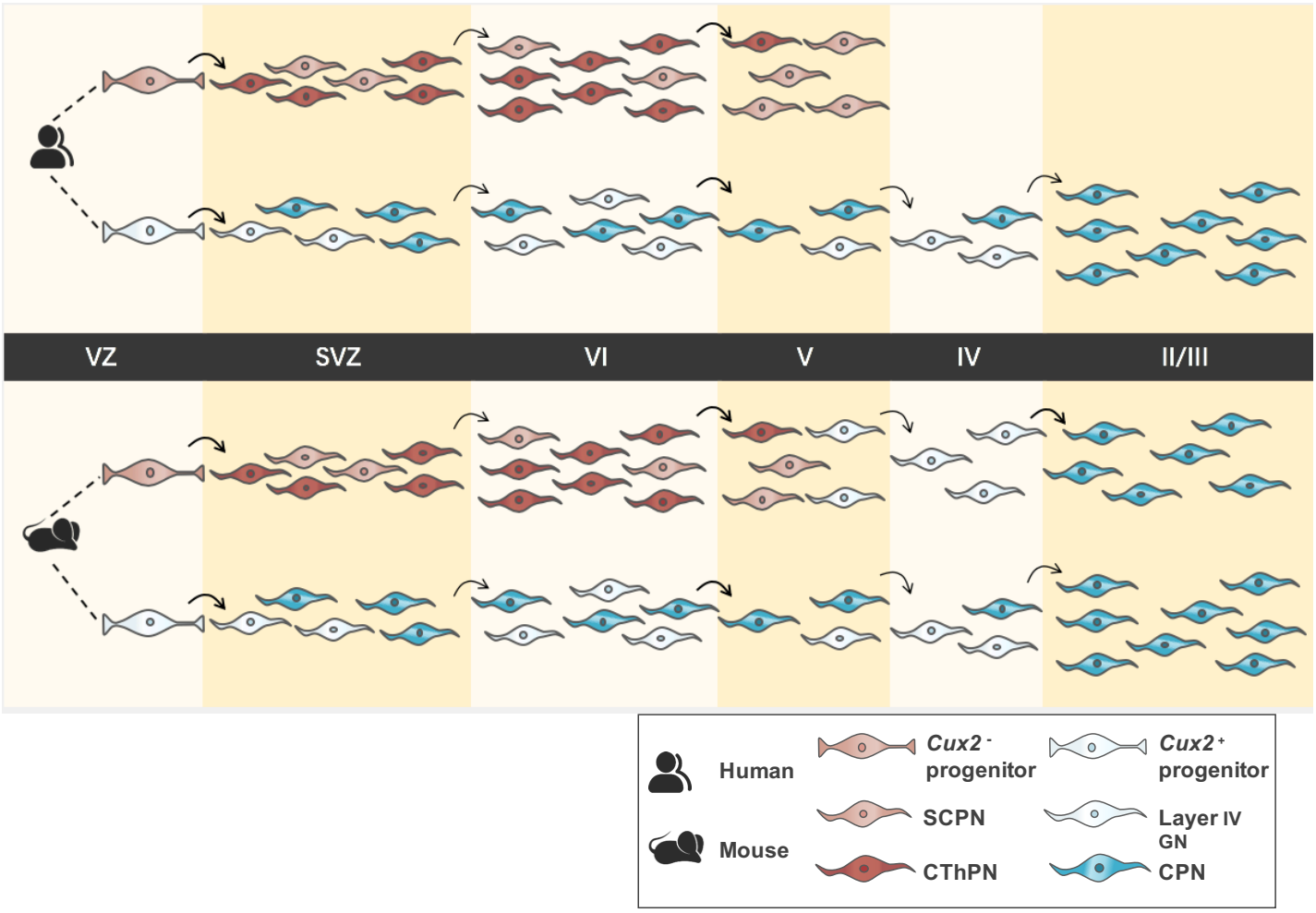
VZ
SVZ
VI
V
IV
II/III
Human
Mouse
Cux2 - progenitor
Cux2 + progenitor
SCPN
Layer IV GN
CThPN
CPN

B

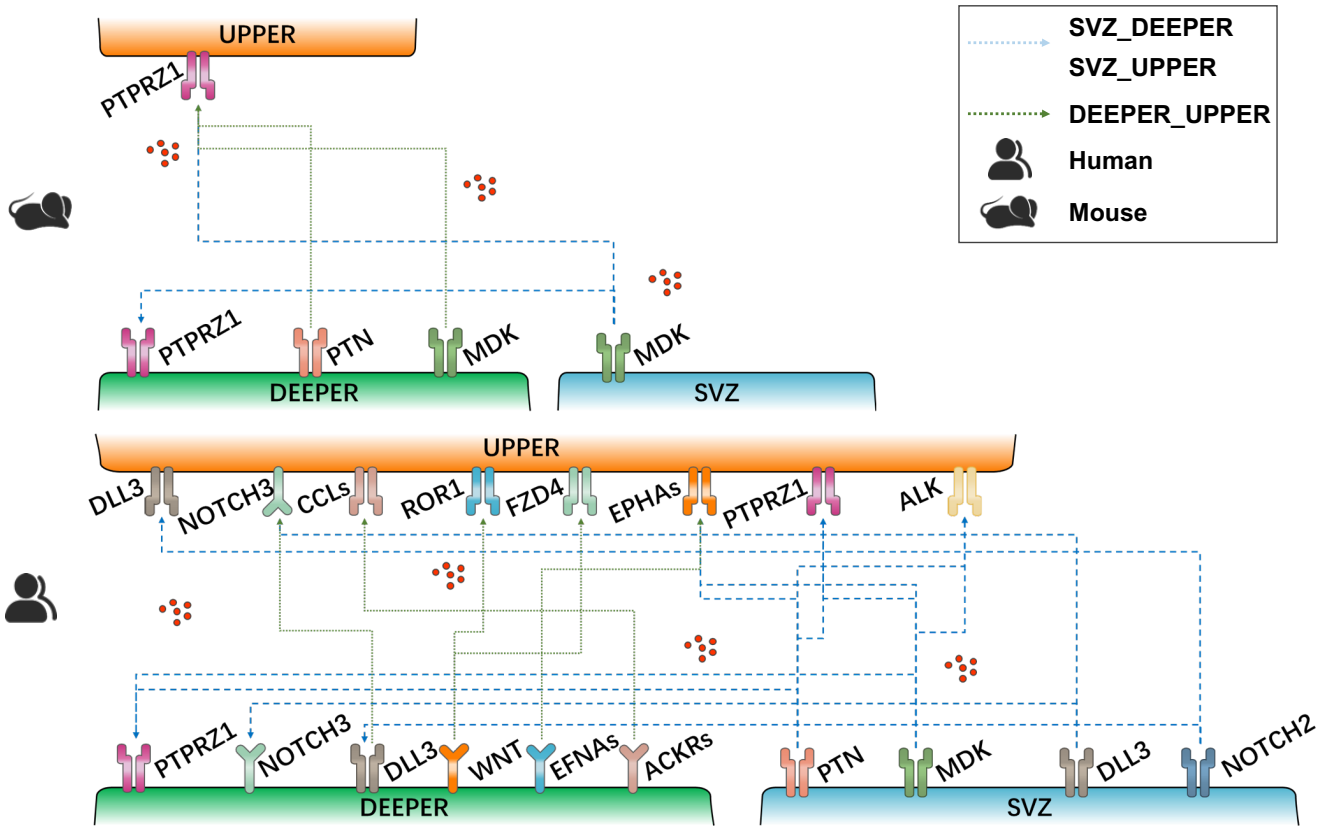
UPPER
PTPRZ1
PTPRZ1
PTN
MDK
MDK
DEEPER
SVZ
UPPER
DLL3
NOTCH3
CCLs
ROR1
FZD4
EPHAs
PTPRZ1
ALK
PTPRZ1
NOTCH3
DLL3
WNT
EFNAs
ACKRs
DEEPER
PTN
MDK
DLL3
NOTCH2
SVZ
SVZ_DEEPER
SVZ_UPPER
DEEPER_UPPER
Human
Mouse

FigureS1

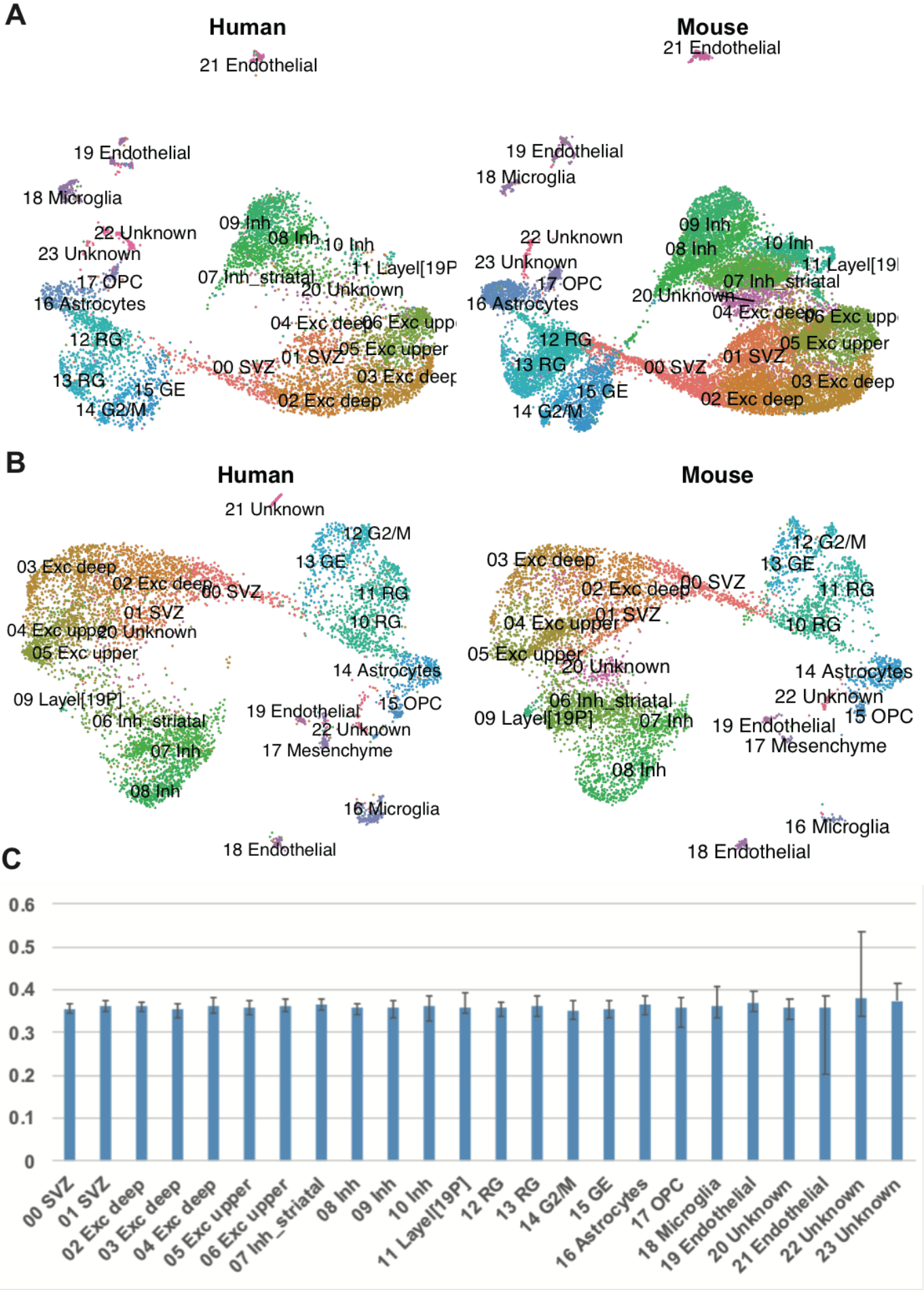
A
Human
21 Endothelial
19 Endothelial
18 Microglia
22 Unknown
23 Unknown
17 OPC
16 Astrocytes
12 RG
13 RG
14 G2/M
15 GE
09 Inh
08 Inh
10 Inh
11 Layel[19P
07 Inh_striatal
20 Unknown
04 Exc deep
06 Exc upp
05 Exc upper
01 SVZ
00 SVZ
03 Exc deep
02 Exc deep
Mouse
21 Endothelial
19 Endothelial
18 Microglia
22 Unknown
23 Unknown
17 OPC
16 Astrocytes
12 RG
13 RG
14 G2/M
15 GE
09 Inh
08 Inh
10 Inh
11 Layel[19
07 Inh_striatal
20 Unknown
04 Exc deep
06 Exc upp
05 Exc upper
01 SVZ
00 SVZ
03 Exc deep
02 Exc deep
B
Human
21 Unknown
12 G2/M
13 GE
03 Exc deep
02 Exc deep
00 SVZ
11 RG
01 SVZ
10 RG
04 Exc upper
20 Unknown
05 Exc upper
14 Astrocytes
09 Layel[19P]
15 OPC
06 Inh_striatal
19 Endothelial
22 Unknown
17 Mesenchyme
07 Inh
08 Inh
16 Microglia
18 Endothelial
Mouse
12 G2/M
13 GE
03 Exc deep
00 SVZ
02 Exc deep
11 RG
01 SVZ
10 RG
04 Exc upper
05 Exc upper
20 Unknown
14 Astrocytes
22 Unknown
06 Inh_striatal
15 OPC
09 Layel[19P]
07 Inh
19 Endothelial
17 Mesenchyme
08 Inh
16 Microglia
18 Endothelial
C
0.6
0.5
0.4
0.3
0.2
0.1
0
00 SVZ
01 SVZ
02 Exc deep
03 Exc deep
04 Exc deep
05 Exc upper
06 Exc upper
07 Inh_striatal
08 Inh
09 Inh
10 Inh
11 Layel[19P]
12 RG
13 RG
14 G2/M
15 GE
16 Astrocytes
17 OPC
18 Microglia
19 Endothelial
20 Unknown
21 Endothelial
22 Unknown
23 Unknown

Figure S2

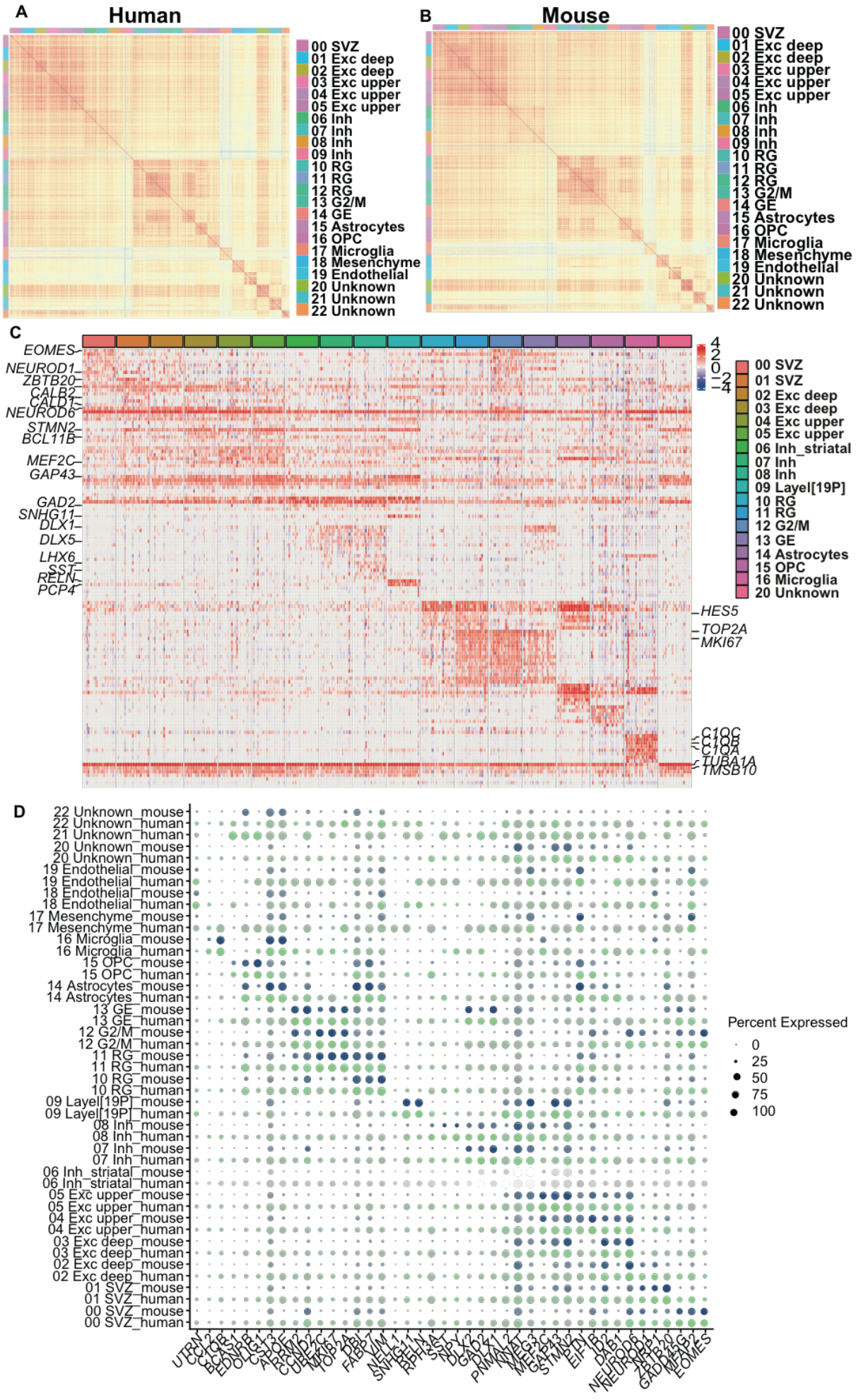
A
Human
00 SVZ
01 Exc deep
02 Exc deep
03 Exc upper
04 Exc upper
05 Exc upper
06 Inh
07 Inh
08 Inh
09 Inh
10 RG
11 RG
12 RG
13 G2/M
14 GE
15 Astrocytes
16 OPC
17 Microglia
18 Mesenchyme
19 Endothelial
20 Unknown
21 Unknown
22 Unknown
B
Mouse
00 SVZ
01 Exc deep
02 Exc deep
03 Exc upper
04 Exc upper
05 Exc upper
06 Inh
07 Inh
08 Inh
09 Inh
10 RG
11 RG
12 RG
13 G2/M
14 GE
15 Astrocytes
16 OPC
17 Microglia
18 Mesenchyme
19 Endothelial
20 Unknown
21 Unknown
22 Unknown
C
EOMES
NEUROD1
ZBTB20
CALB2
CALD1
NEUROD6
STMN2
BCL11B
MEF2C
GAP43
GAD2
SNHG11
DLX1
DLX5
LHX6
SST
RELN
PCP4
HES5
TOP2A
MKI67
C1QC
C1QB
C1QA
TUBA1A
TMSB10
4
2
0
−2
−4
00 SVZ
01 SVZ
02 Exc deep
03 Exc deep
04 Exc upper
05 Exc upper
06 Inh_striatal
07 Inh
08 Inh
09 Layel[19P]
10 RG
11 RG
12 G2/M
13 GE
14 Astrocytes
15 OPC
16 Microglia
20 Unknown
D
22 Unknown_mouse
22 Unknown_human
21 Unknown_human
20 Unknown_mouse
20 Unknown_human
19 Endothelial_mouse
19 Endothelial_human
18 Endothelial_mouse
18 Endothelial_human
17 Mesenchyme_mouse
17 Mesenchyme_human
16 Microglia_mouse
16 Microglia_human
15 OPC_mouse
15 OPC_human
14 Astrocytes_mouse
14 Astrocytes_human
13 GE_mouse
13 GE_human
12 G2/M_mouse
12 G2/M_human
11 RG_mouse
11 RG_human
10 RG_mouse
10 RG_human
09 Layel[19P]_mouse
09 Layel[19P]_human
08 Inh_mouse
08 Inh_human
07 Inh_mouse
07 Inh_human
06 Inh_striatal_mouse
06 Inh_striatal_human
05 Exc upper_mouse
05 Exc upper_human
04 Exc upper_mouse
04 Exc upper_human
03 Exc deep_mouse
03 Exc deep_human
02 Exc deep_mouse
02 Exc deep_human
01 SVZ_mouse
01 SVZ_human
00 SVZ_mouse
00 SVZ_human
UTRN
CCL2
C1QB
BCAS1
EDNRB
COL13A1
APOE
PRM2
CCND2
CUX2
MKI67
TOP2A
FABP7
VIM
NEU1
SNHG11
RELN
RPH3A
SST
NPY
DLX2
GAD2
DLX1
PRMT2
NNAT
MEF2C
MEGF3
STMN2
PDYN
EIF1B
ID2
DAB1
NEUROD6
NEUROD1
ZBTB20
GADD45G
MEF2D
EOMES
Percent Expressed
0
25
50
75
100

Figure S3

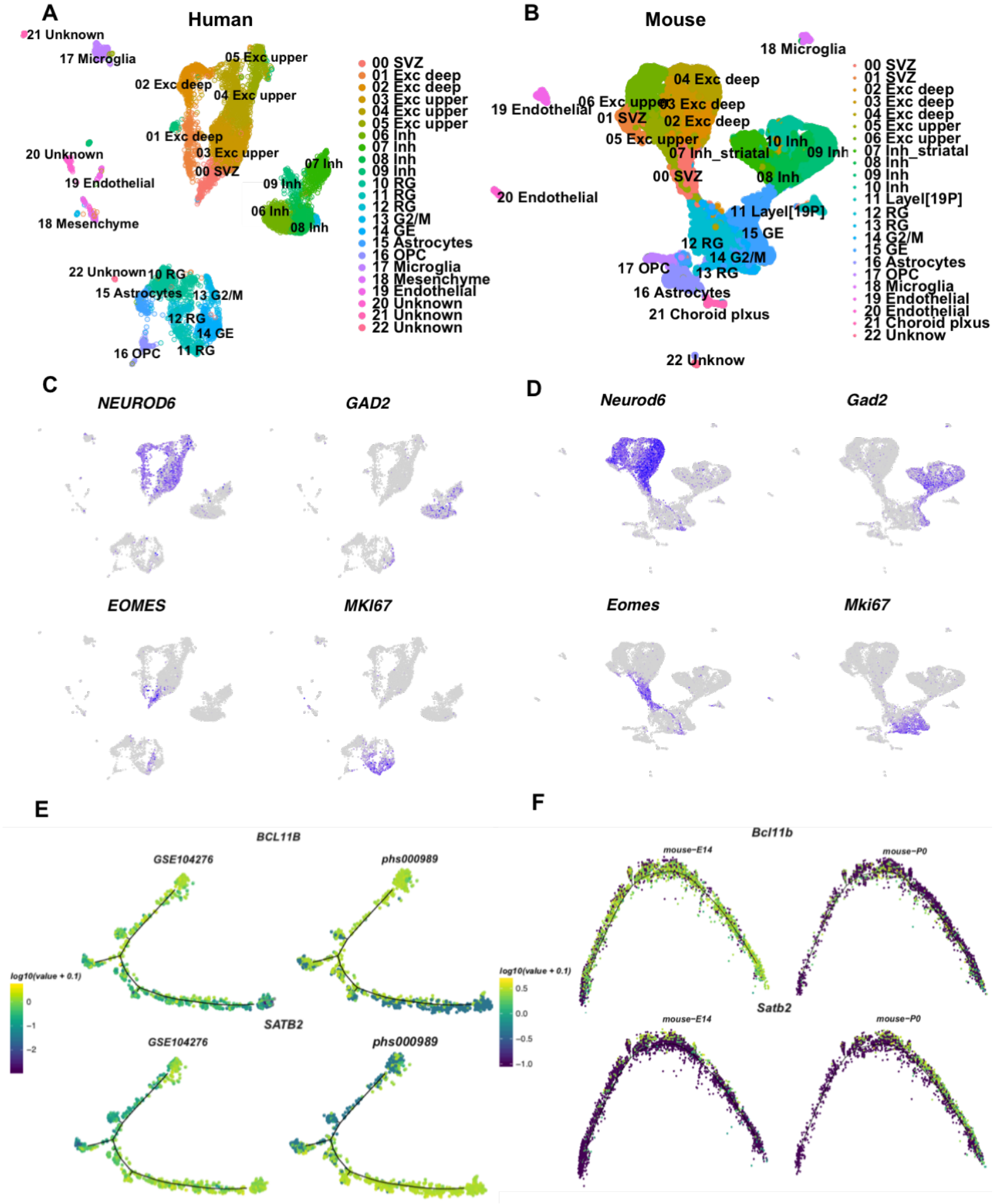
A
Human
21 Unknown
17 Microglia
05 Exc upper
02 Exc deep
04 Exc upper
01 Exc deep
03 Exc upper
00 SVZ
20 Unknown
19 Endothelial
18 Mesenchyme
07 Inh
09 Inh
06 Inh
08 Inh
22 Unknown
10 RG
15 Astrocytes
13 G2/M
12 RG
14 GE
16 OPC
11 RG
00 SVZ
01 Exc deep
02 Exc deep
03 Exc upper
04 Exc upper
05 Exc upper
06 Inh
07 Inh
08 Inh
09 Inh
10 RG
11 RG
12 RG
13 G2/M
14 GE
15 Astrocytes
16 OPC
17 Microglia
18 Mesenchyme
19 Endothelial
20 Unknown
21 Unknown
22 Unknown
B
Mouse
18 Microglia
04 Exc deep
19 Endothelial
06 Exc upper
03 Exc deep
01 SVZ
02 Exc deep
05 Exc upper
10 Inh
09 Inh
07 Inh_striatal
00 SVZ
08 Inh
20 Endothelial
11 Layel[19P]
15 GE
12 RG
14 G2/M
17 OPC
13 RG
16 Astrocytes
21 Choroid plxus
22 Unknow
00 SVZ
01 SVZ
02 Exc deep
03 Exc deep
04 Exc deep
05 Exc upper
06 Exc upper
07 Inh_striatal
08 Inh
09 Inh
10 Inh
11 Layel[19P]
12 RG
13 RG
14 G2/M
15 GE
16 Astrocytes
17 OPC
18 Microglia
19 Endothelial
20 Endothelial
21 Choroid plxus
22 Unknow
C
NEUROD6
GAD2
EOMES
MKI67
D
Neurod6
Gad2
Eomes
Mki67
E
BCL11B
GSE104276
phs000989
log10(value + 0.1)
0
−1
−2
SATB2
GSE104276
phs000989
F
Bcl11b
mouse−E14
mouse−P0
log10(value + 0.1)
0.5
0.0
−0.5
−1.0
Satb2
mouse−E14
mouse−P0

Figure S3

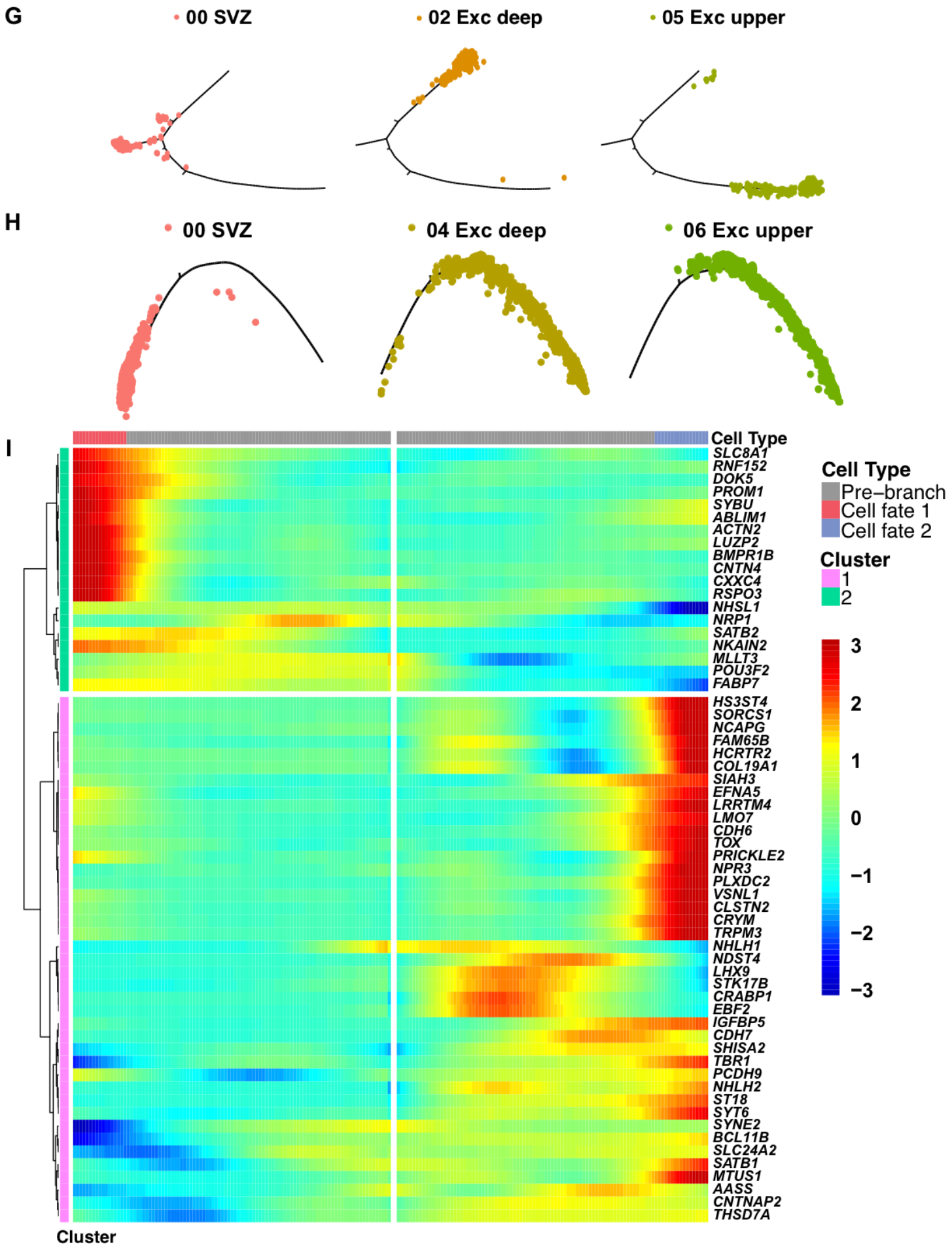
G
00 SVZ
02 Exc deep
05 Exc upper
H
00 SVZ
04 Exc deep
06 Exc upper
I
Cell Type
SLC8A1
RNF152
DOK5
PROM1
SYBU
ABLIM1
ACTN2
LUZP2
BMPR1B
CNTN4
CXXC4
RSPO3
NHSL1
NRP1
SATB2
NKAIN2
MLLT3
POU3F2
FABP7
HS3ST4
SORCS1
NCAPG
FAM65B
HCRTR2
COL19A1
SIAH3
EFNA5
LRRTM4
LMO7
CDH6
TOX
PRICKLE2
NPR3
PLXDC2
VSNL1
CLSTN2
CRYM
TRPM3
NHLH1
NDST4
LHX9
STK17B
CRABP1
EBF2
IGFBP5
CDH7
SHISA2
TBR1
PCDH9
NHLH2
ST18
SYT6
SYNE2
BCL11B
SLC24A2
SATB1
MTUS1
AASS
CNTNAP2
THSD7A
Cluster
Cell Type
Pre–branch
Cell fate 1
Cell fate 2
Cluster
1
2
3
2
1
0
−1
−2
−3

Figure S3

J

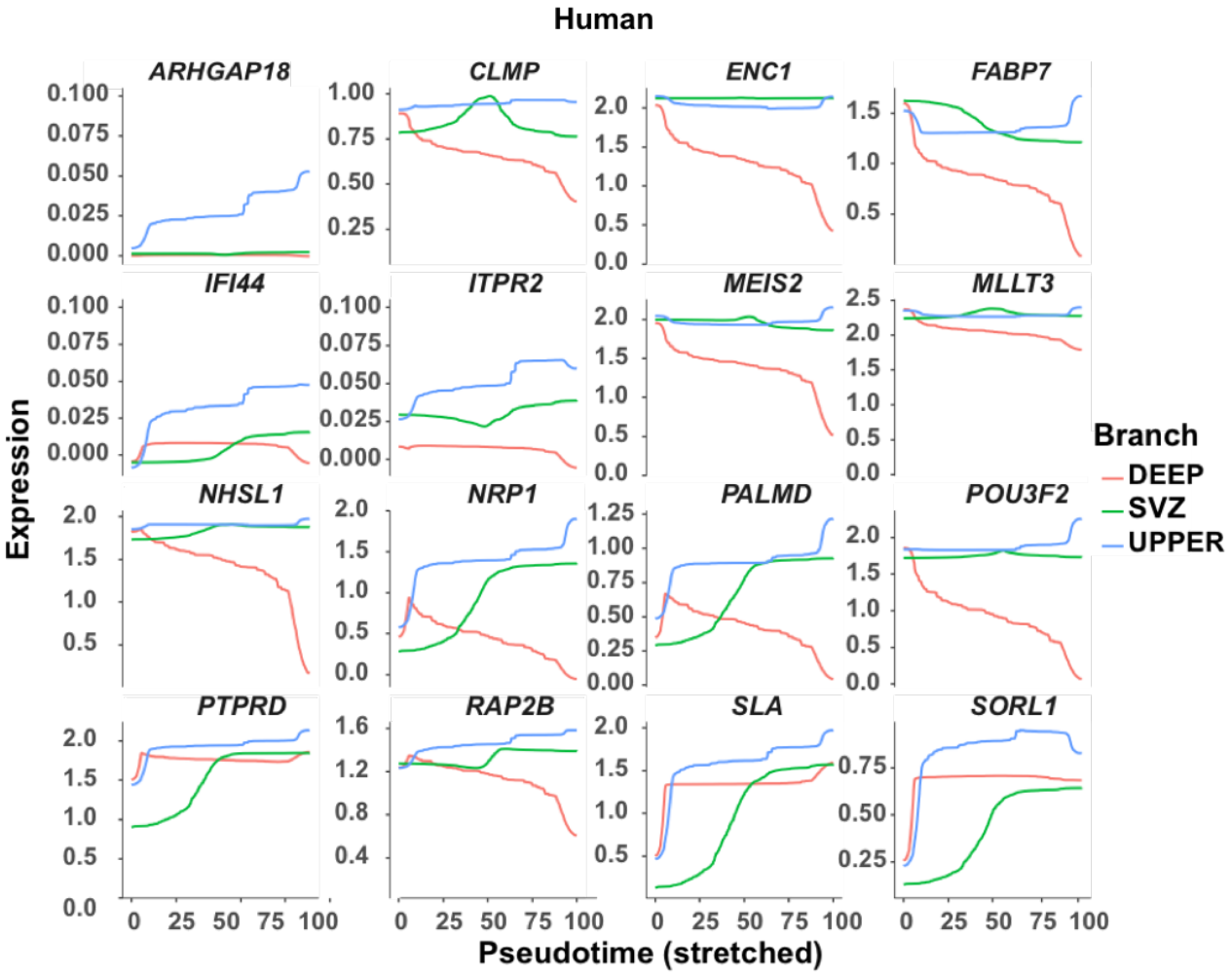
Human
ARHGAP18
CLMP
ENC1
FABP7
IFI44
ITPR2
MEIS2
MLLT3
NHSL1
NRP1
PALMD
POU3F2
PTPRD
RAP2B
SLA
SORL1
Expression
Pseudotime (stretched)
Branch
DEEP
SVZ
UPPER

K

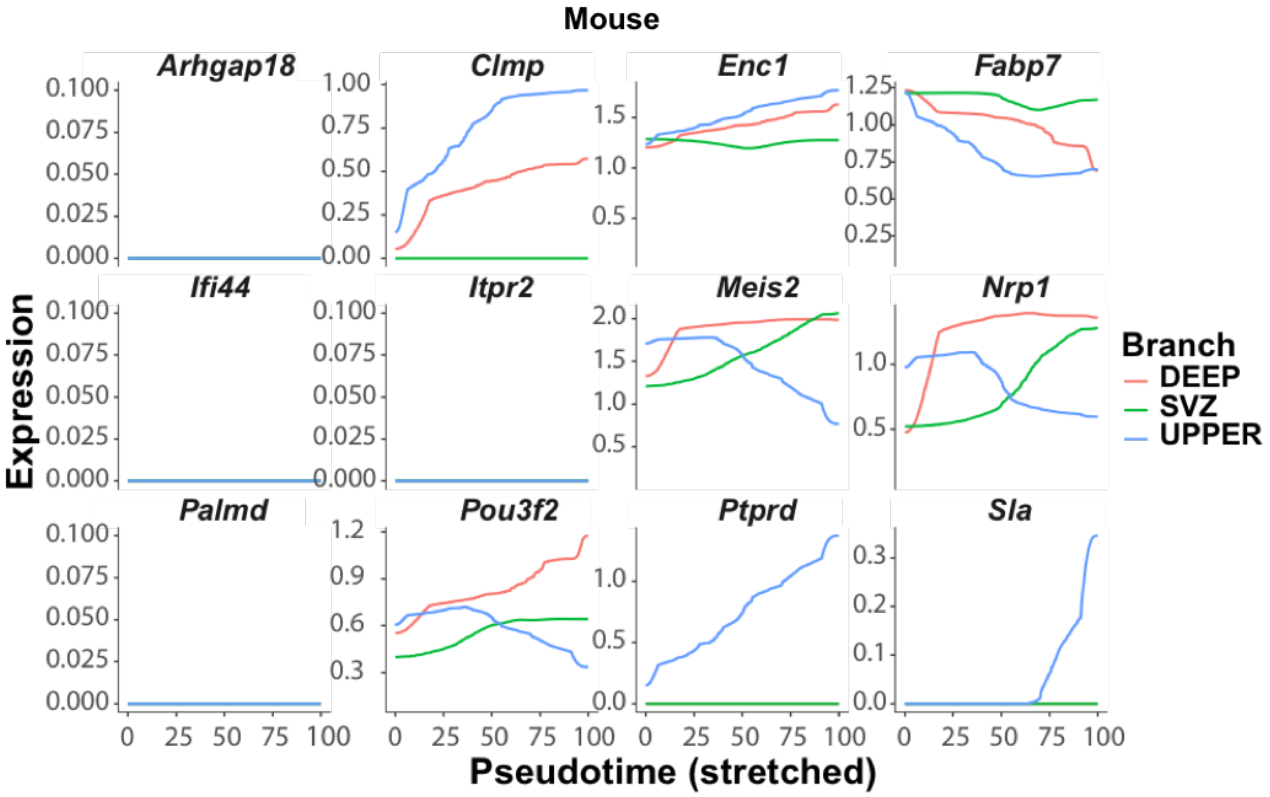
Mouse
Arhgap18
Clmp
Enc1
Fabp7
Ifi44
Itpr2
Meis2
Nrp1
Palmd
Pou3f2
Ptprd
Sla
Expression
Pseudotime (stretched)
Branch
DEEP
SVZ
UPPER

Figure S4

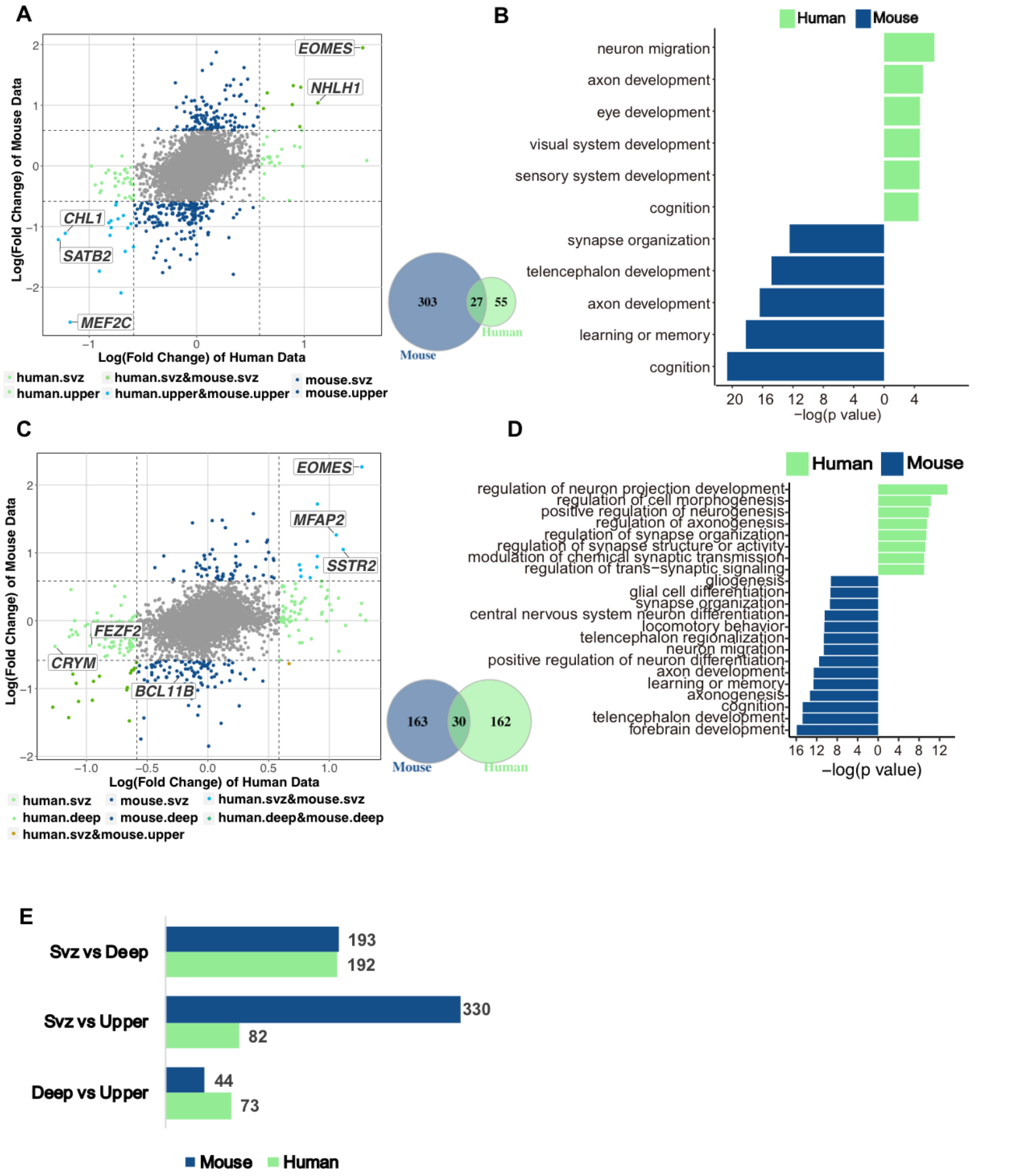
A
EOMES
NHLH1
CHL1
SATB2
MEF2C
Log(Fold Change) of Mouse Data
Log(Fold Change) of Human Data
human.svz
human.svz&mouse.svz
mouse.svz
human.upper
human.upper&mouse.upper
mouse.upper
303
27
55
Mouse
Human
B
Human
Mouse
neuron migration
axon development
eye development
visual system development
sensory system development
cognition
synapse organization
telencephalon development
axon development
learning or memory
cognition
−log(p value)
C
EOMES
MFAP2
SSTR2
FEZF2
CRYM
BCL11B
Log(Fold Change) of Mouse Data
Log(Fold Change) of Human Data
human.svz
mouse.svz
human.svz&mouse.svz
human.deep
mouse.deep
human.deep&mouse.deep
human.svz&mouse.upper
163
30
162
Mouse
Human
D
Human
Mouse
regulation of neuron projection development
regulation of cell morphogenesis
positive regulation of neurogenesis
regulation of axonogenesis
regulation of synapse organization
regulation of synapse structure or activity
modulation of chemical synaptic transmission
regulation of trans−synaptic signaling
gliogenesis
glial cell differentiation
synapse organization
central nervous system neuron differentiation
locomotory behavior
telencephalon regionalization
neuron migration
positive regulation of neuron differentiation
axon development
learning or memory
axonogenesis
cognition
telencephalon development
forebrain development
−log(p value)
E
Svz vs Deep
193
192
Svz vs Upper
330
82
Deep vs Upper
44
73
Mouse
Human

Figure S5

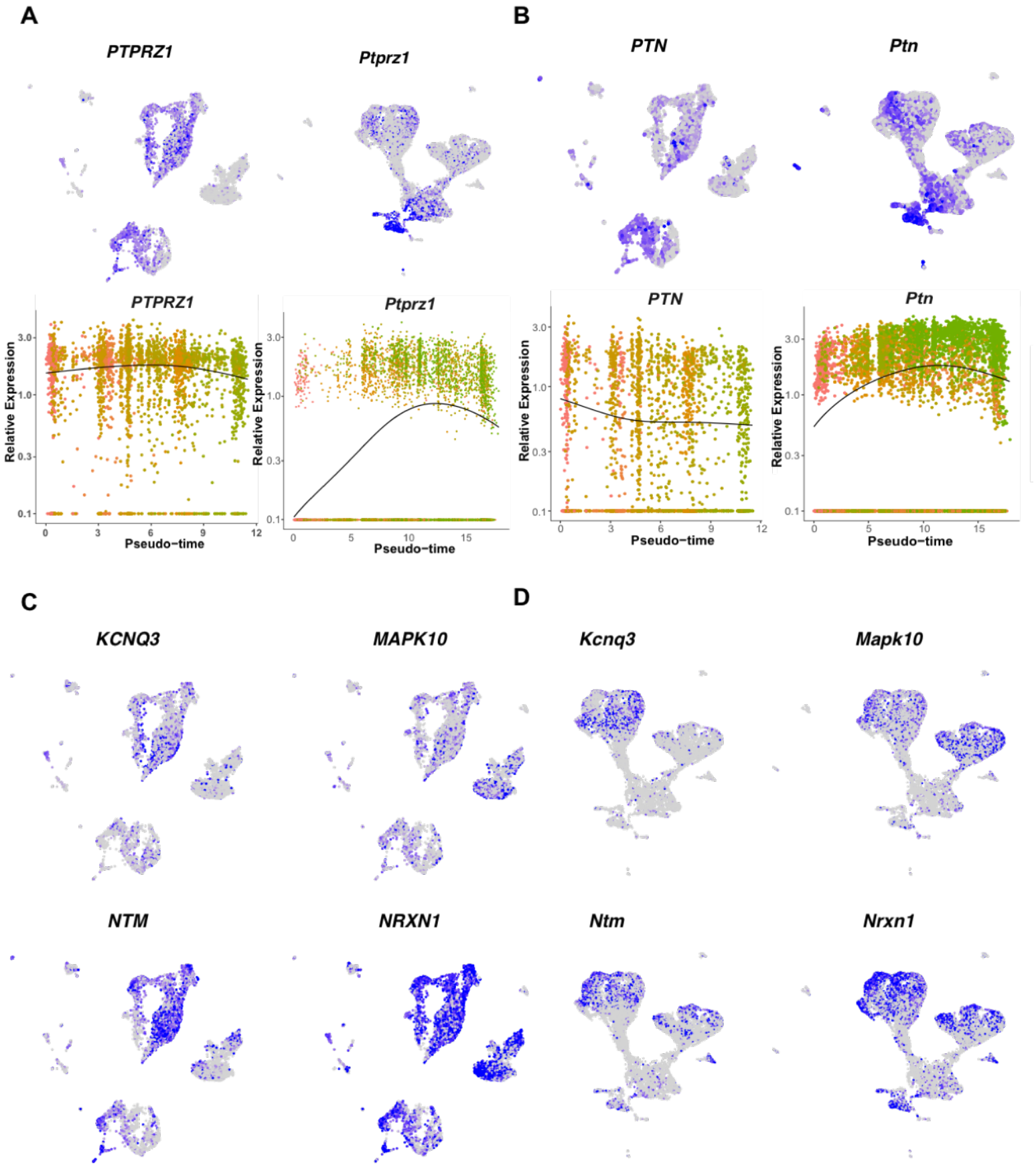
A
PTPRZ1
Ptprz1
PTPRZ1
Ptprz1
Relative Expression
Pseudo−time
B
PTN
Ptn
PTN
Ptn
Relative Expression
Pseudo−time
C
KCNQ3
MAPK10
NTM
NRXN1
D
Kcnq3
Mapk10
Ntm
Nrxn1

Figure S5

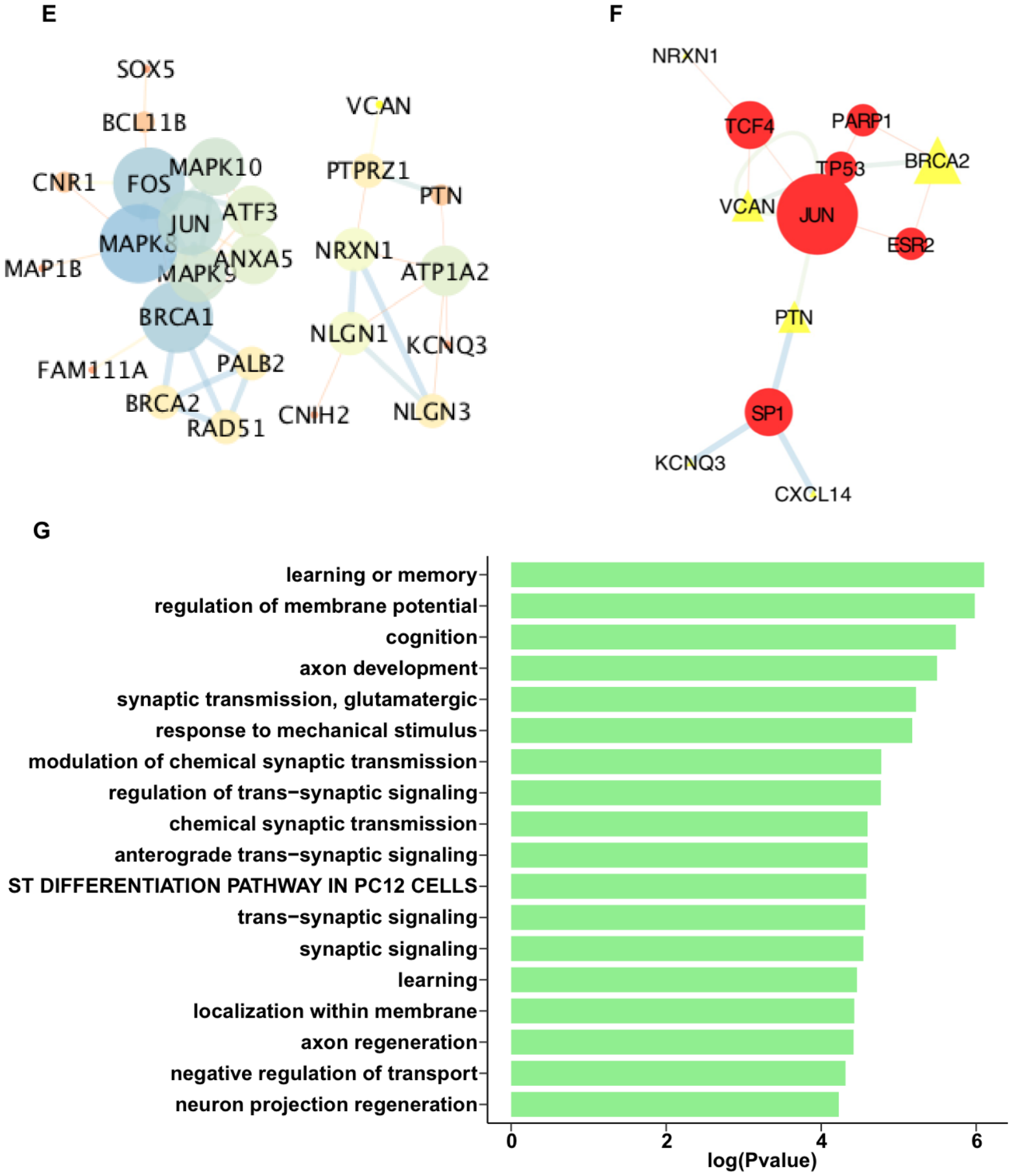
E
SOX5
BCL11B
VCAN
CNR1
FOS
MAPK10
PTPRZ1
PTN
ATF3
JUN
MAPK8
ANXA5
NRXN1
MAP1B
MAPK9
ATP1A2
BRCA1
NLGN1
KCNQ3
FAM111A
PALB2
BRCA2
CNIH2
NLGN3
RAD51
F
NRXN1
TCF4
PARP1
TP53
BRCA2
VCAN
JUN
ESR2
PTN
SP1
KCNQ3
CXCL14
G
learning or memory
regulation of membrane potential
cognition
axon development
synaptic transmission, glutamatergic
response to mechanical stimulus
modulation of chemical synaptic transmission
regulation of trans−synaptic signaling
chemical synaptic transmission
anterograde trans−synaptic signaling
ST DIFFERENTIATION PATHWAY IN PC12 CELLS
trans−synaptic signaling
synaptic signaling
learning
localization within membrane
axon regeneration
negative regulation of transport
neuron projection regeneration
0
2
4
6
log(Pvalue)

Figure S6

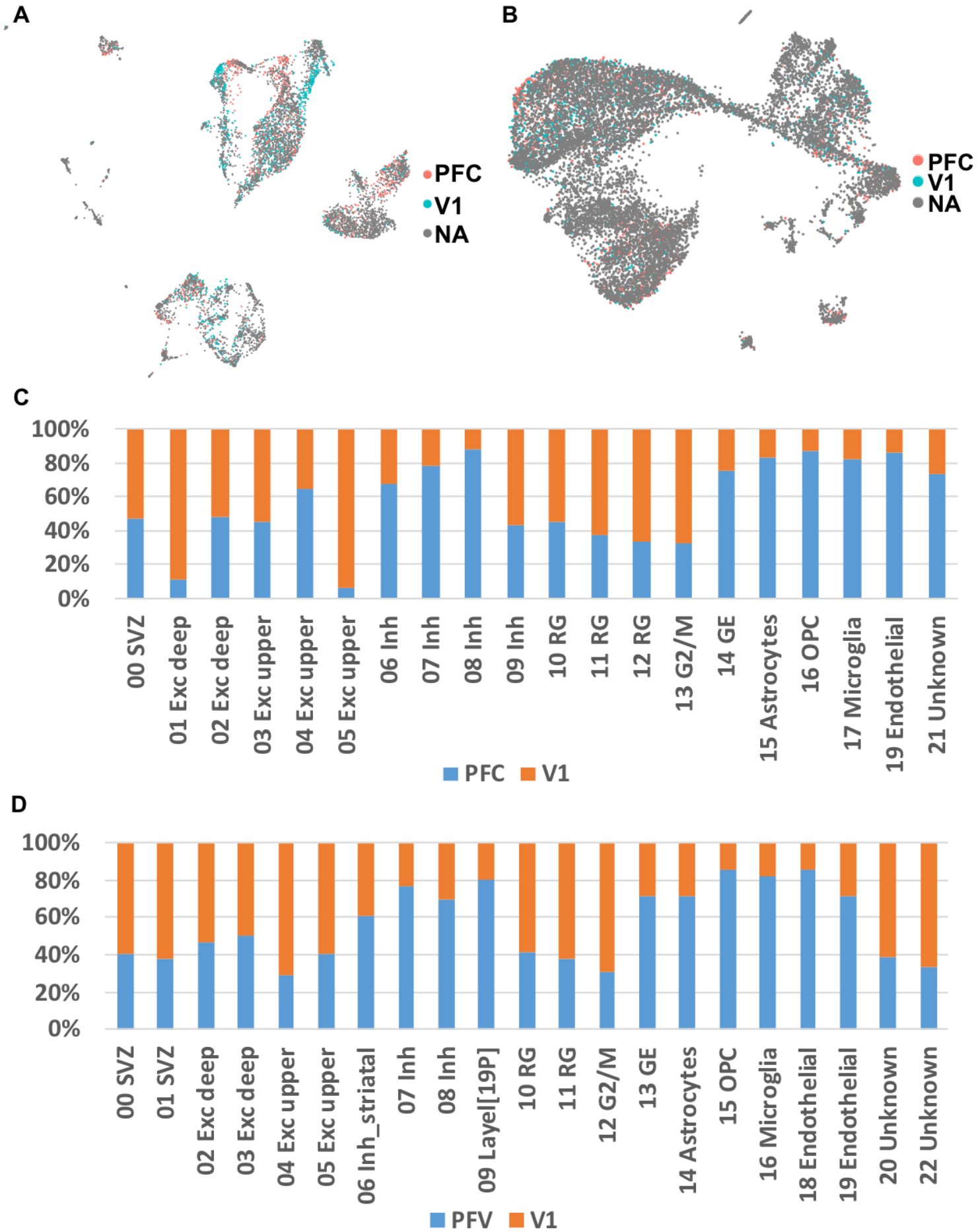
A
PFC
V1
NA
B
PFC
V1
NA
C
100%
80%
60%
40%
20%
0%
00 SVZ
01 Exc deep
02 Exc deep
03 Exc upper
04 Exc upper
05 Exc upper
06 Inh
07 Inh
08 Inh
09 Inh
10 RG
11 RG
12 RG
13 G2/M
14 GE
15 Astrocytes
16 OPC
17 Microglia
19 Endothelial
21 Unknown
PFC
V1
D
100%
80%
60%
40%
20%
0%
00 SVZ
01 SVZ
02 Exc deep
03 Exc deep
04 Exc upper
05 Exc upper
06 Inh_striatal
07 Inh
08 Inh
09 Layel[19P]
10 RG
11 RG
12 G2/M
13 GE
14 Astrocytes
15 OPC
16 Microglia
18 Endothelial
19 Endothelial
20 Unknown
22 Unknown
PFV
V1

Figure S7

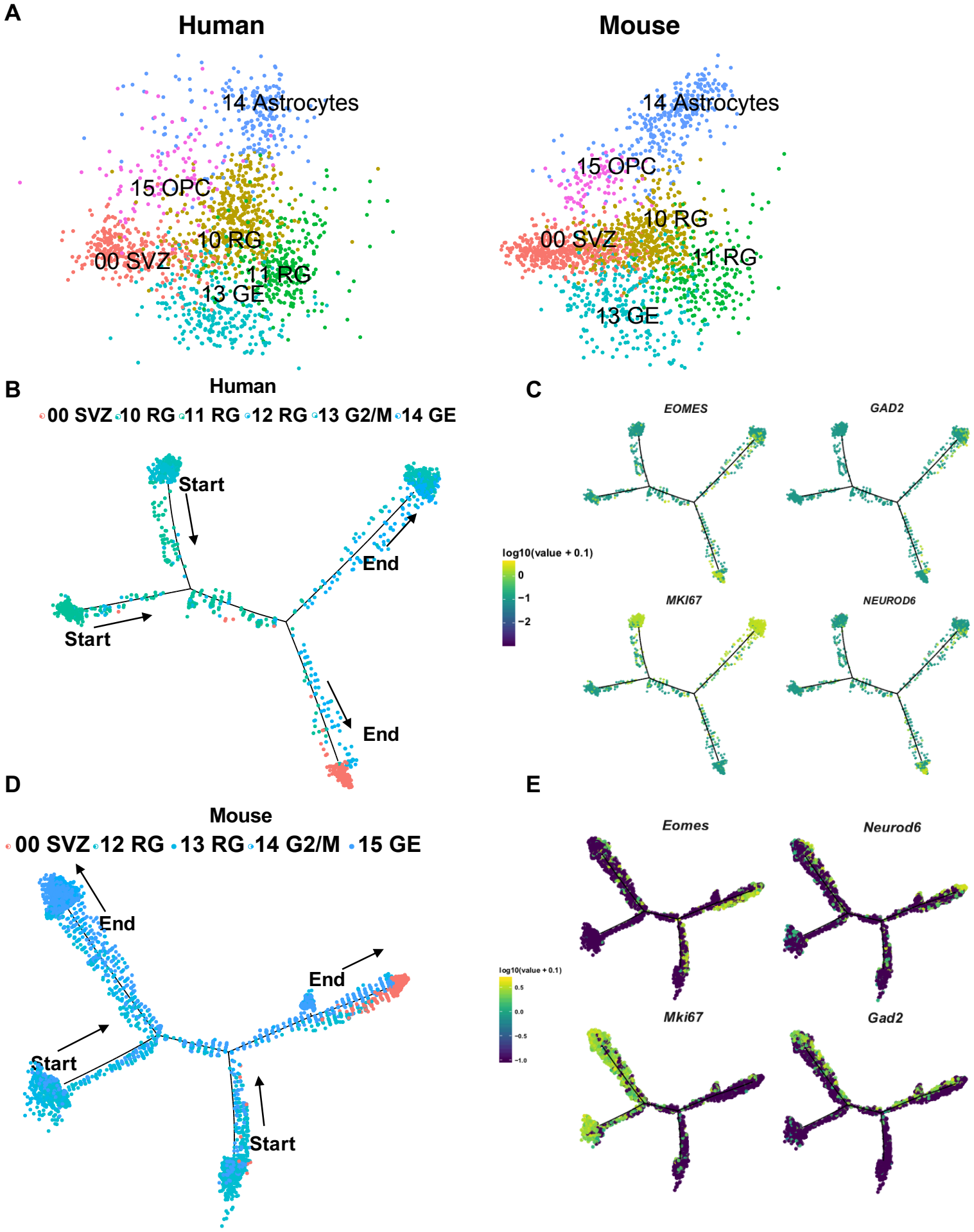
A
Human
14 Astrocytes
15 OPC
10 RG
00 SVZ
11 RG
13 GE
Mouse
14 Astrocytes
15 OPC
10 RG
00 SVZ
11 RG
13 GE
B
Human
00 SVZ 10 RG 11 RG 12 RG 13 G2/M 14 GE
Start
End
Start
End
C
EOMES
GAD2
log10(value + 0.1)
0
−1
−2
MKI67
NEUROD6
D
Mouse
00 SVZ 12 RG 13 RG 14 G2/M 15 GE
End
End
Start
Start
E
Eomes
Neurod6
log10(value + 0.1)
0.5
0.0
−0.5
−1.0
Mki67
Gad2

Figure S7

F

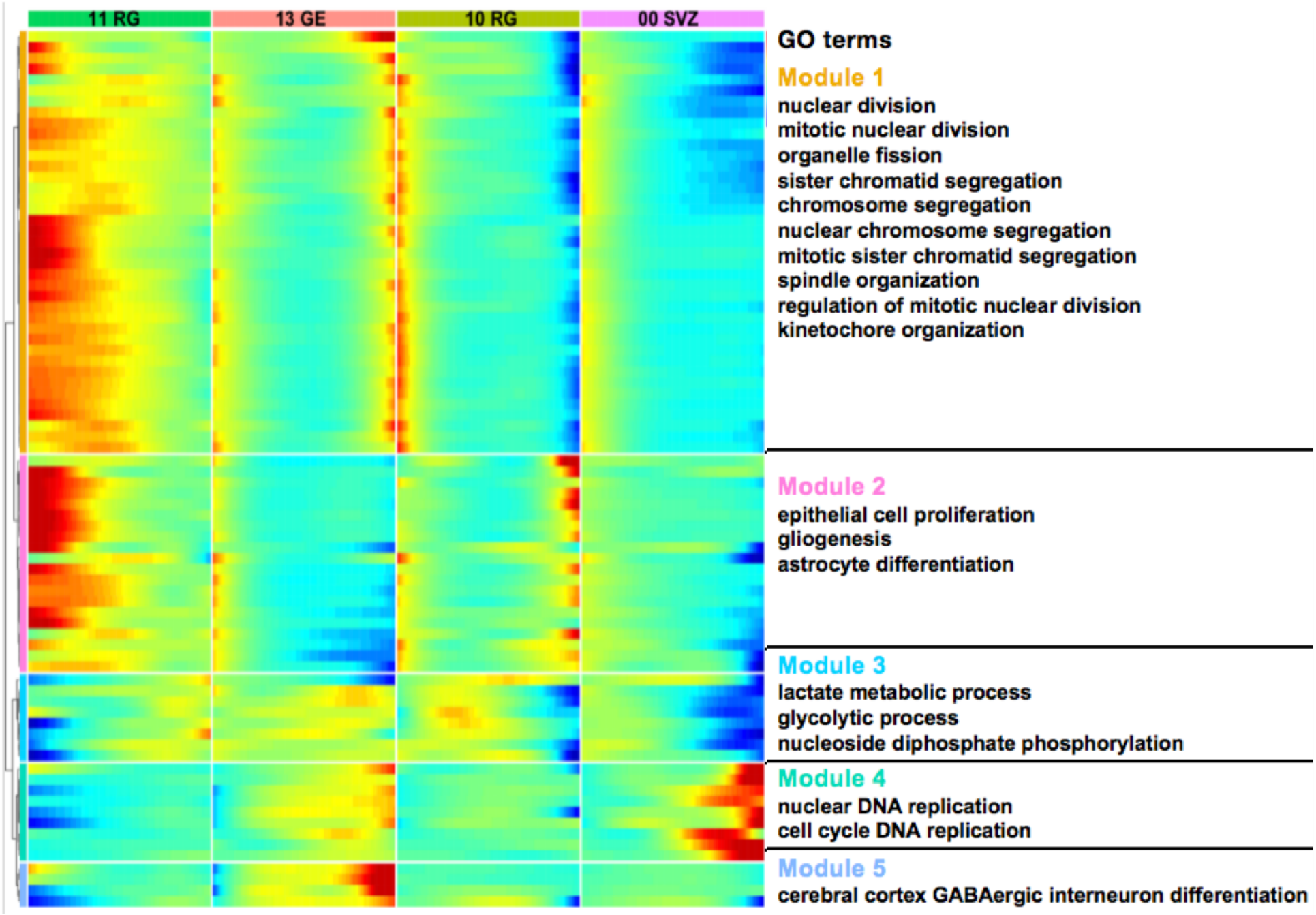
11 RG
13 GE
10 RG
00 SVZ
GO terms
Module 1
nuclear division
mitotic nuclear division
organelle fission
sister chromatid segregation
chromosome segregation
nuclear chromosome segregation
mitotic sister chromatid segregation
spindle organization
regulation of mitotic nuclear division
kinetochore organization
Module 2
epithelial cell proliferation
gliogenesis
astrocyte differentiation
Module 3
lactate metabolic process
glycolytic process
nucleoside diphosphate phosphorylation
Module 4
nuclear DNA replication
cell cycle DNA replication
Module 5
cerebral cortex GABAergic interneuron differentiation

Figure S8

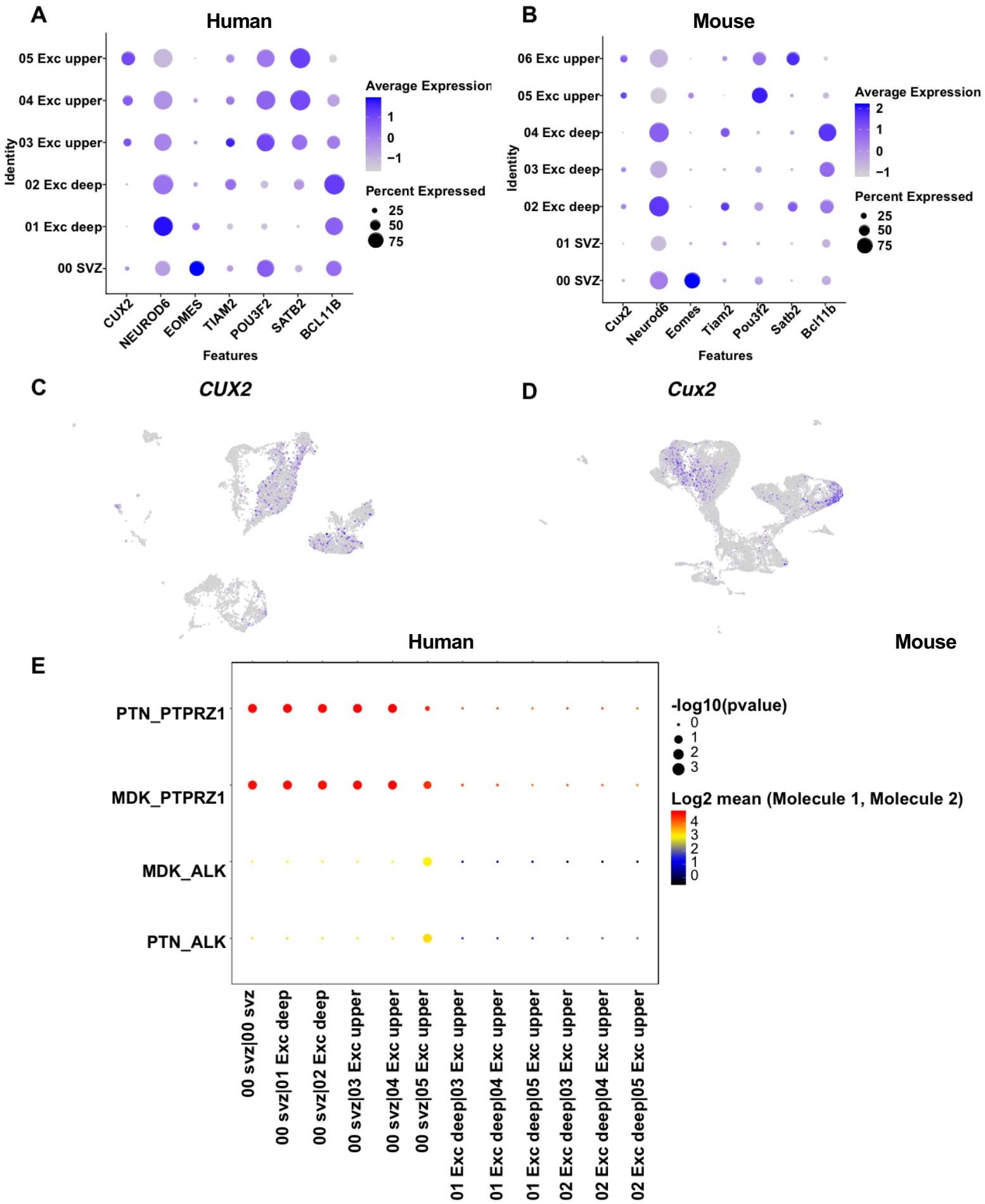
A
Human
05 Exc upper
04 Exc upper
03 Exc upper
02 Exc deep
01 Exc deep
00 SVZ
Identity
CUX2
NEUROD6
EOMES
TIAM2
POU3F2
SATB2
BCL11B
Features
Average Expression
1
0
−1
Percent Expressed
25
50
75
B
Mouse
06 Exc upper
05 Exc upper
04 Exc deep
03 Exc deep
02 Exc deep
01 SVZ
00 SVZ
Identity
Cux2
Neurod6
Eomes
Tiam2
Pou3f2
Satb2
Bcl11b
Features
Average Expression
2
1
0
−1
Percent Expressed
25
50
75
C
CUX2
D
Cux2
E
Human
Mouse
PTN_PTPRZ1
MDK_PTPRZ1
MDK_ALK
PTN_ALK
00 svz|00 svz
00 svz|01 Exc deep
00 svz|02 Exc deep
00 svz|03 Exc upper
00 svz|04 Exc upper
00 svz|05 Exc upper
01 Exc deep|03 Exc upper
01 Exc deep|04 Exc upper
01 Exc deep|05 Exc upper
02 Exc deep|03 Exc upper
02 Exc deep|04 Exc upper
02 Exc deep|05 Exc upper
-log10(pvalue)
0
1
2
3
Log2 mean (Molecule 1, Molecule 2)
4
3
2
1
0

Figure S8

F

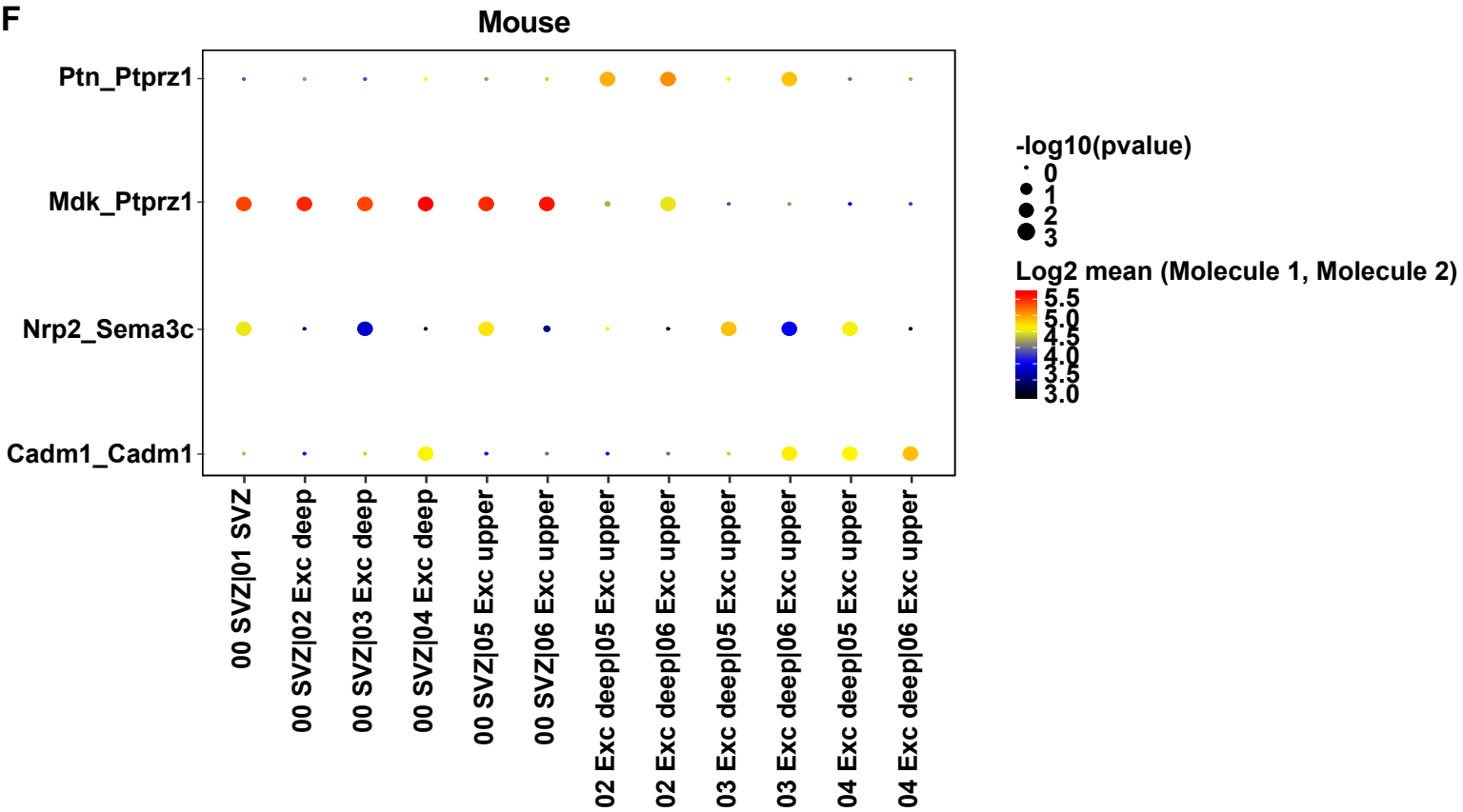
Mouse
Ptn_Ptprz1
Mdk_Ptprz1
Nrp2_Sema3c
Cadm1_Cadm1
00 SVZ|01 SVZ
00 SVZ|02 Exc deep
00 SVZ|03 Exc deep
00 SVZ|04 Exc deep
00 SVZ|05 Exc upper
00 SVZ|06 Exc upper
02 Exc deep|05 Exc upper
02 Exc deep|06 Exc upper
03 Exc deep|05 Exc upper
03 Exc deep|06 Exc upper
04 Exc deep|05 Exc upper
04 Exc deep|06 Exc upper
-log10(pvalue)
0
1
2
3
Log2 mean (Molecule 1, Molecule 2)
5.5
5.0
4.5
4.0
3.5
3.0

G

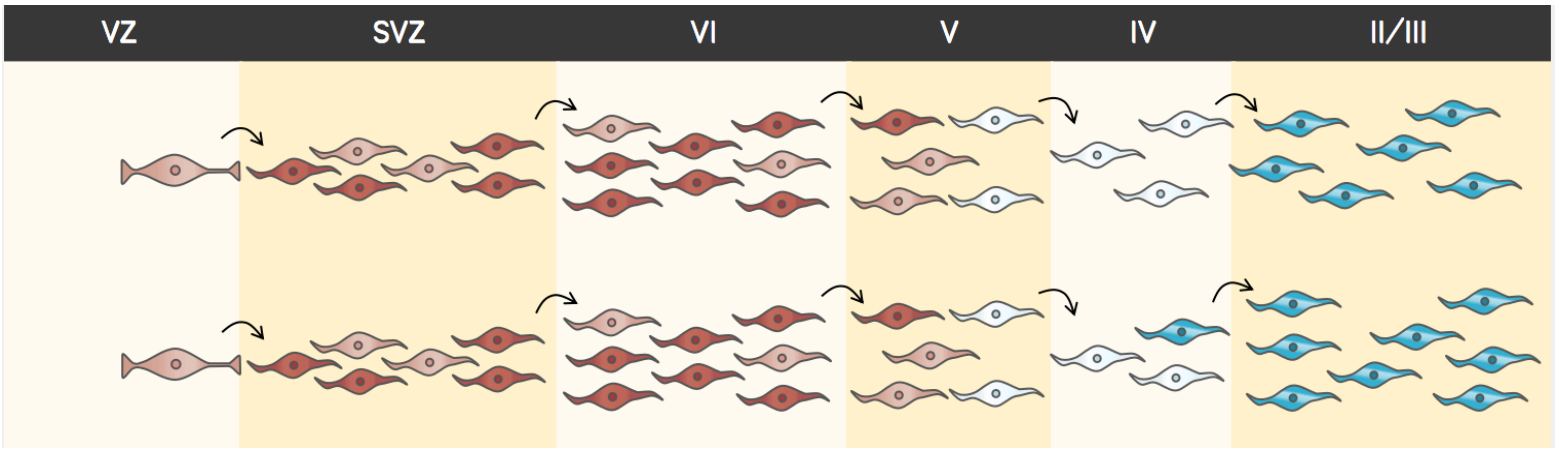
VZ
SVZ
VI
V
IV
II/III